Next-Generation CMB Experiments and Technology

Helmuth Spieler

Lawrence Berkeley National Laboratory
Berkeley, CA 94720

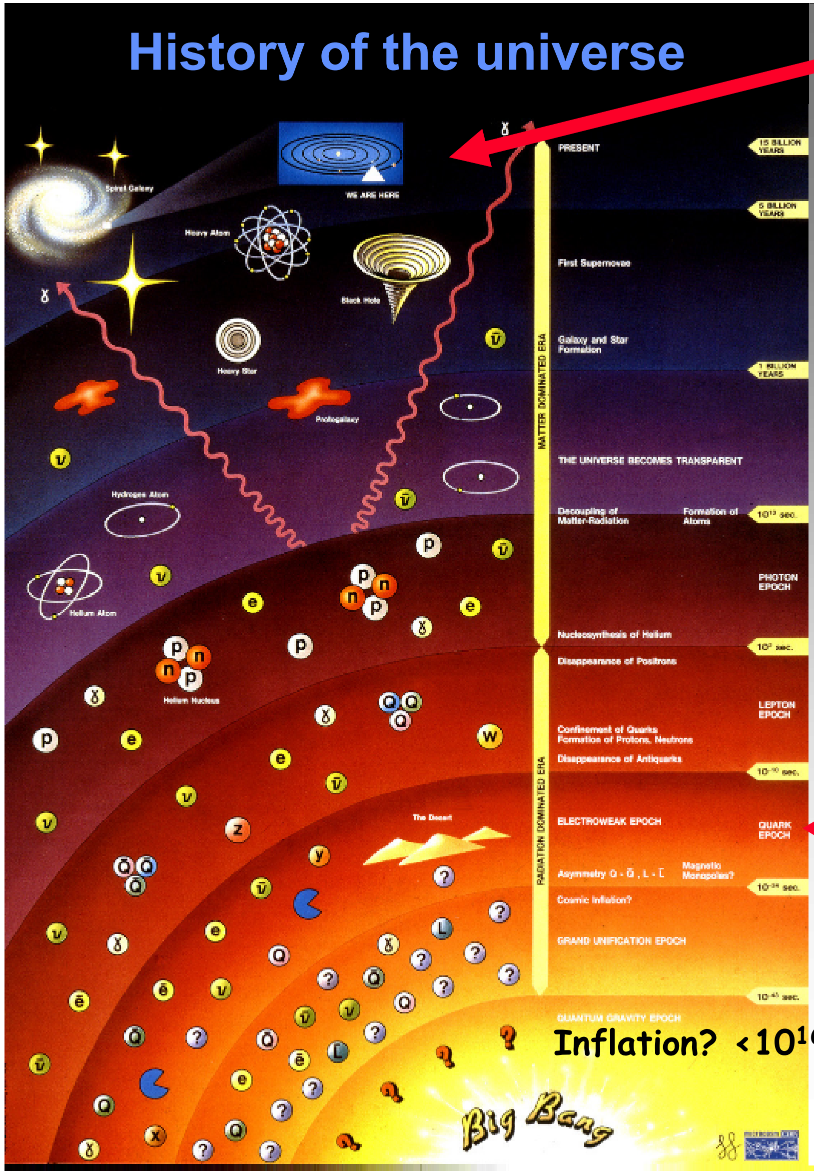

Inflation? $<10^{16}$ GeV

You are here

←NOW (12.7 Billion years)

←Stars form (1 Billion years)

CMB Structure Imprinted

←Atoms Form (300 000 years)

←Nuclei Form (180 seconds)

←Protons and Neutrons Form (10^{-10} sec)

←Quarks Differentiate (10^{-34} sec ?)

LHC probes physics relevant to the universe at age 10^{-14} sec.

Inflation

- At ~10^{-38} s after the Big Bang, the universe undergoes a phase transition causing an explosive 10^{30}-fold exponential expansion
- Leaves its imprint as inflationary gravity waves

Inflation predicts

- Cosmic Microwave Background radiation
- CMB is isotropic
- Exponential expansion locally flattens spatial curvature to high precision.
    - Universe is “flat” (Euclidian geometry)
- Density perturbations, which will eventually collapse under the pull of gravity to produce galaxies, stars,..

CMB has a near perfect black body spectrum (T= 2.7K)

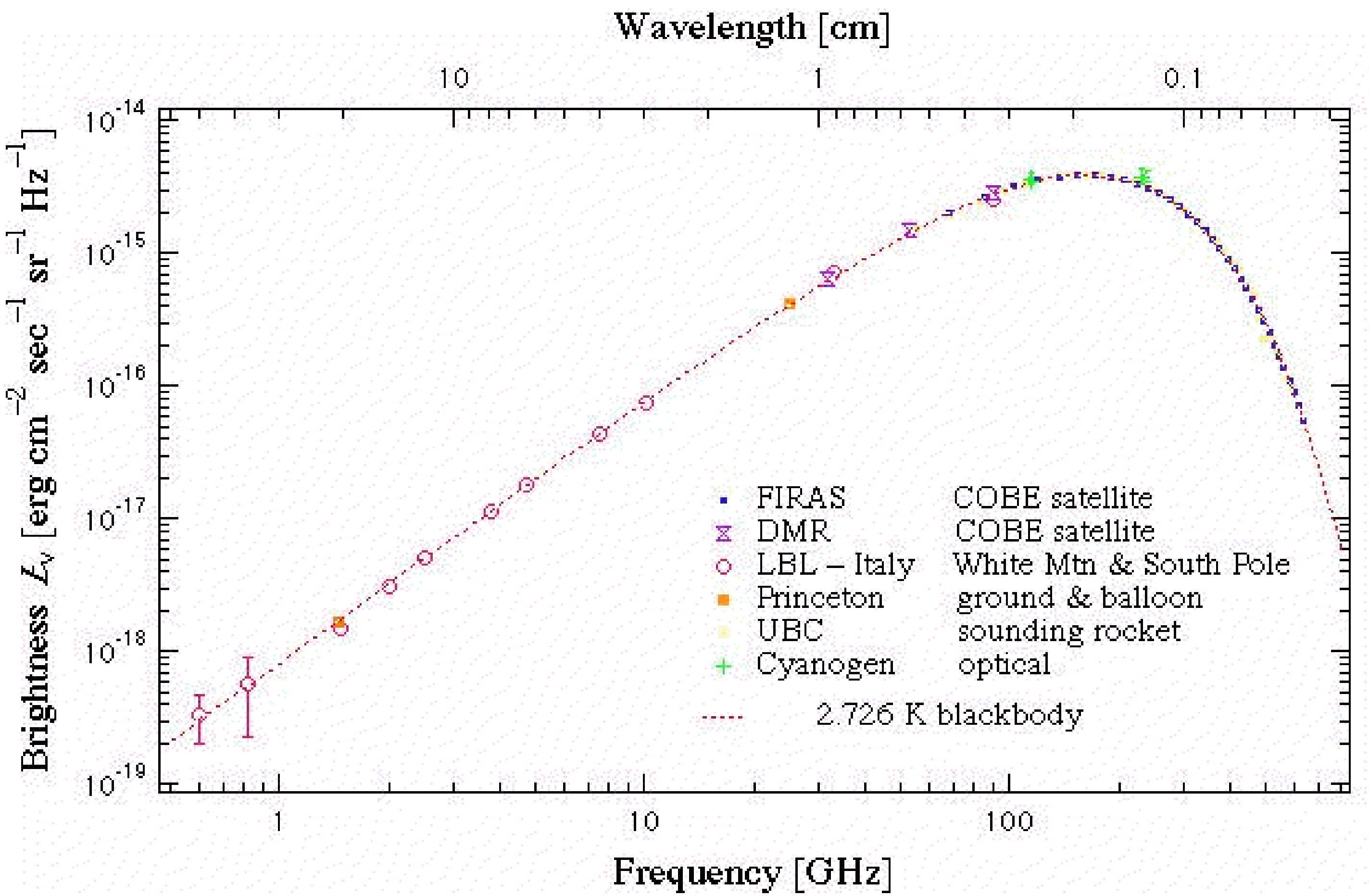

Map Temperature of Sky:

Data from WMAP

Temperature anisotropy ~10^{-5}

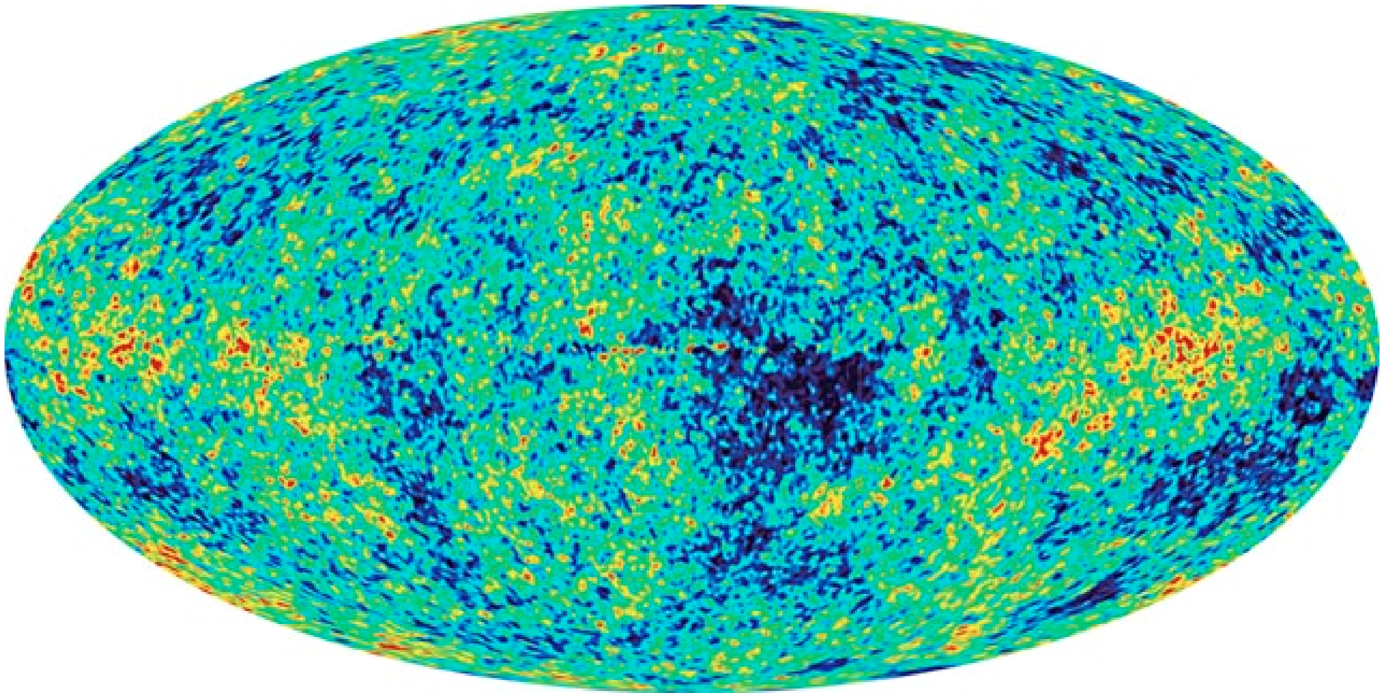

Multipole expansion of spatial distribution – determine angular scales

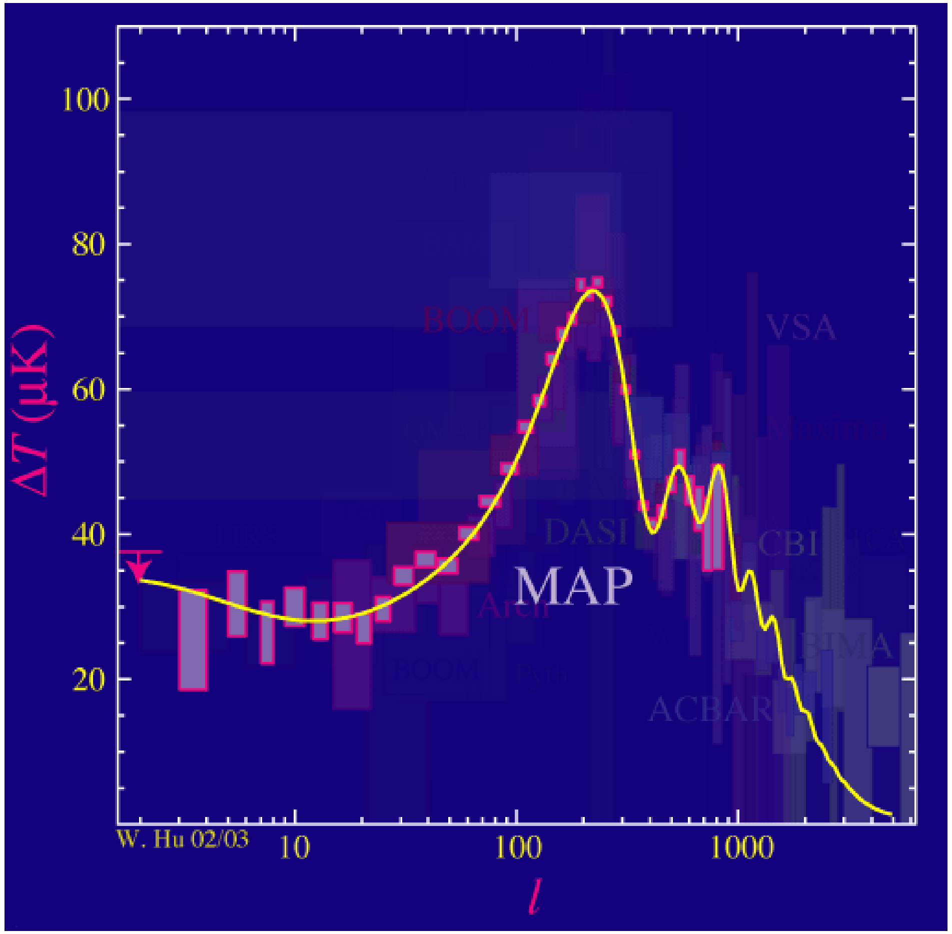

angular resolution $\Delta\Theta \approx 180/\, l$

Angular structure depends on cosmological parameters

For example, geometry:
dominant angular scale ~1°

$\Rightarrow$ universe is flat

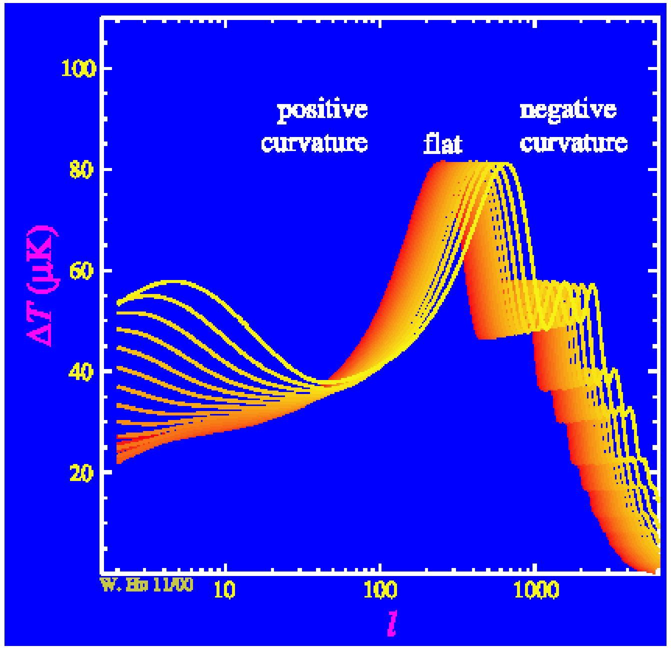

Analyzing the power spectrum:

Normalization set by the total amount of matter $\Omega_M = \Omega_b + \Omega_{CDM}$

Position of 1st peak: geometry of universe

$$
\begin{array}{lll}
l > 200 & \Omega_0 > 1 & \text{pos. curv.} \\
l \approx 200 & \Omega_0 = 1 & \text{flat} \\
l < 200 & \Omega_0 < 1 & \text{neg. curv.}
\end{array}
$$

Ratio of 1st to 2nd peak: amount of baryonic matter

3rd peak > 2nd peak: presence of cold dark matter

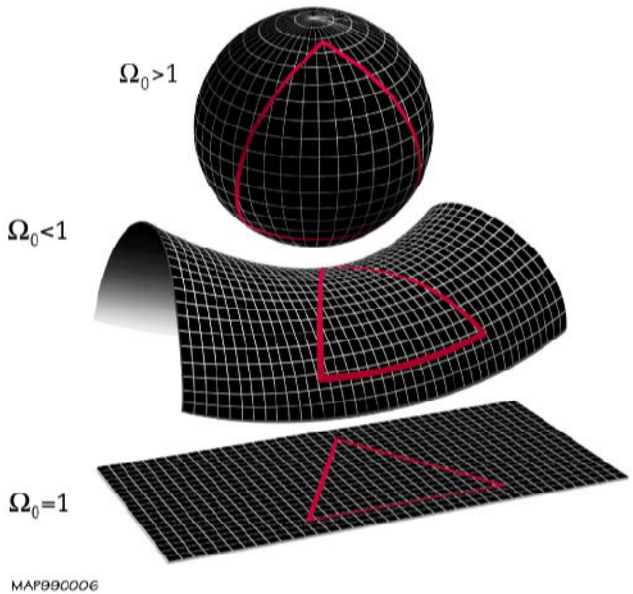

- CMB measurements provide constraints on fundamental cosmological parameters
- CMB spatial distribution largely unaffected since 300k yrs after Big Bang
- Supernova and CMB data *together* give best constraints on mass and energy density of the universe

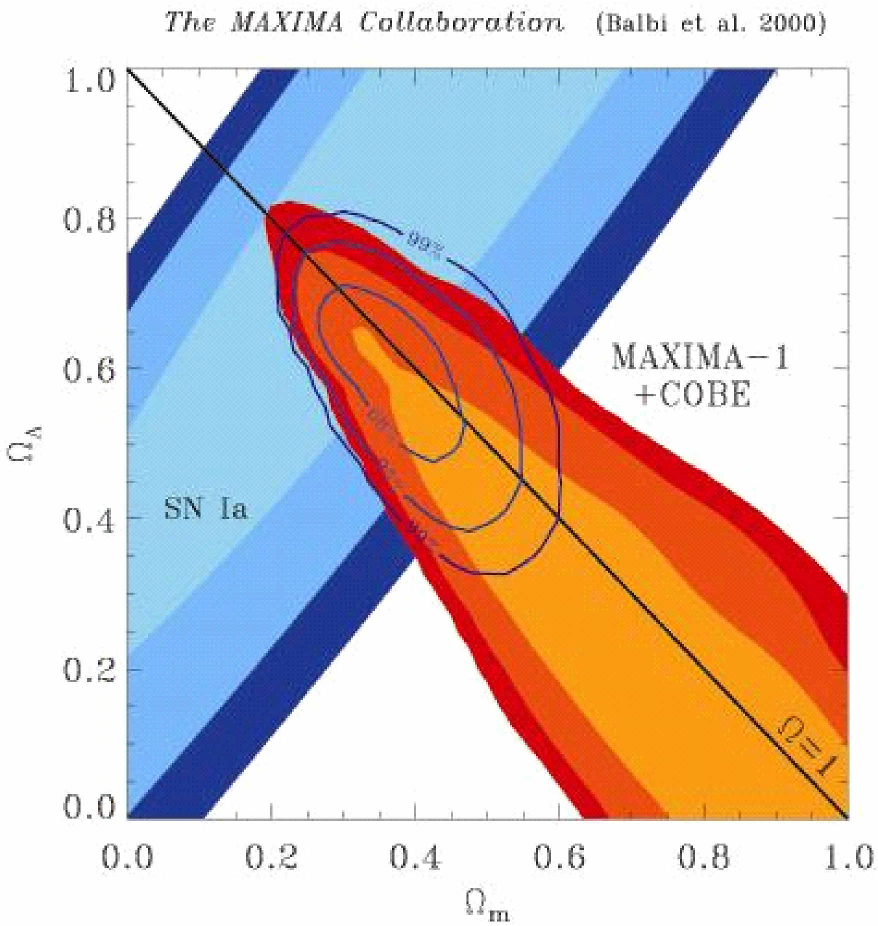

Ground-based Experiments – Example: the Viper telescope at the South Pole

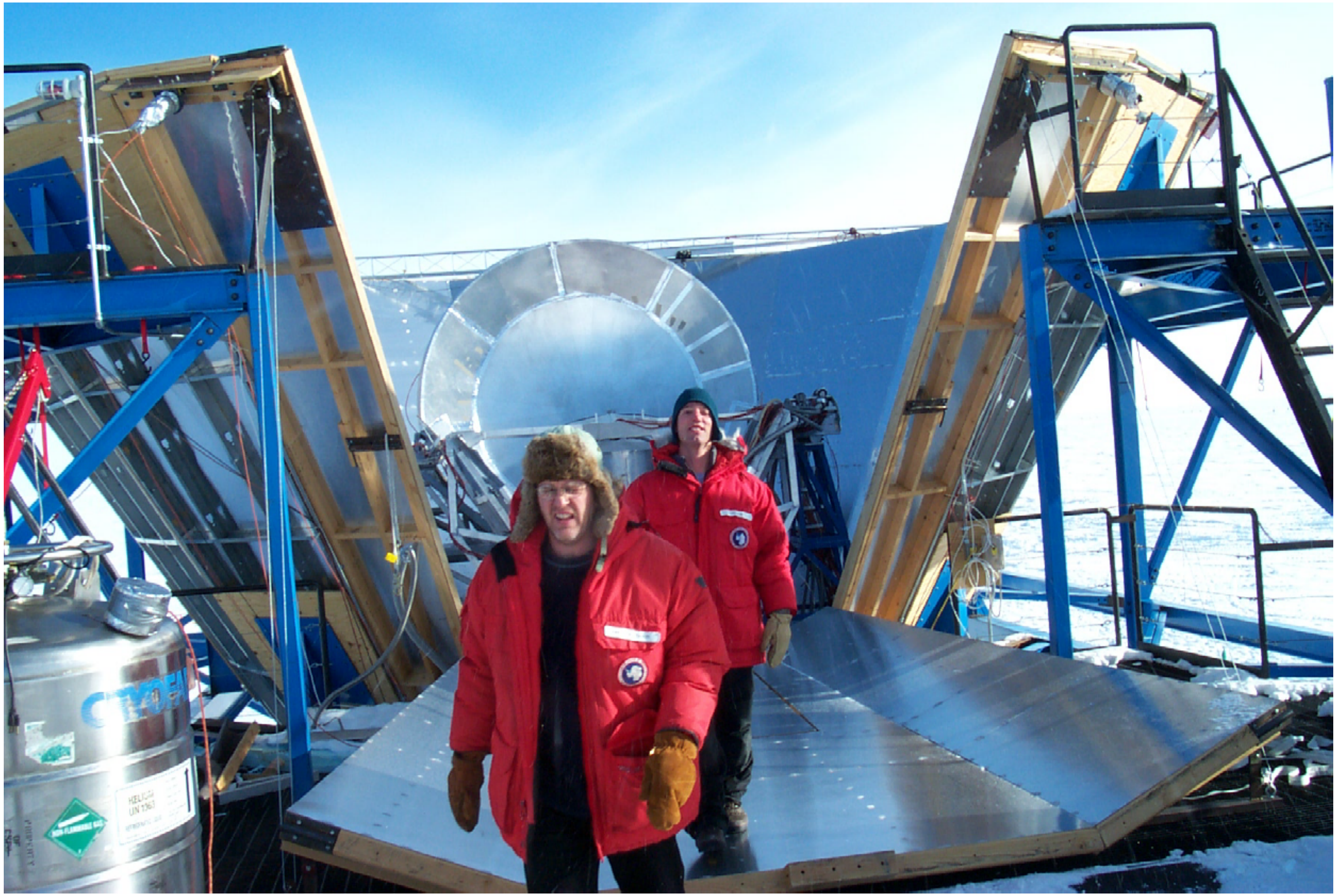

ACBAR focal plane array installed in Viper telescope
(Holzapfel et al.)

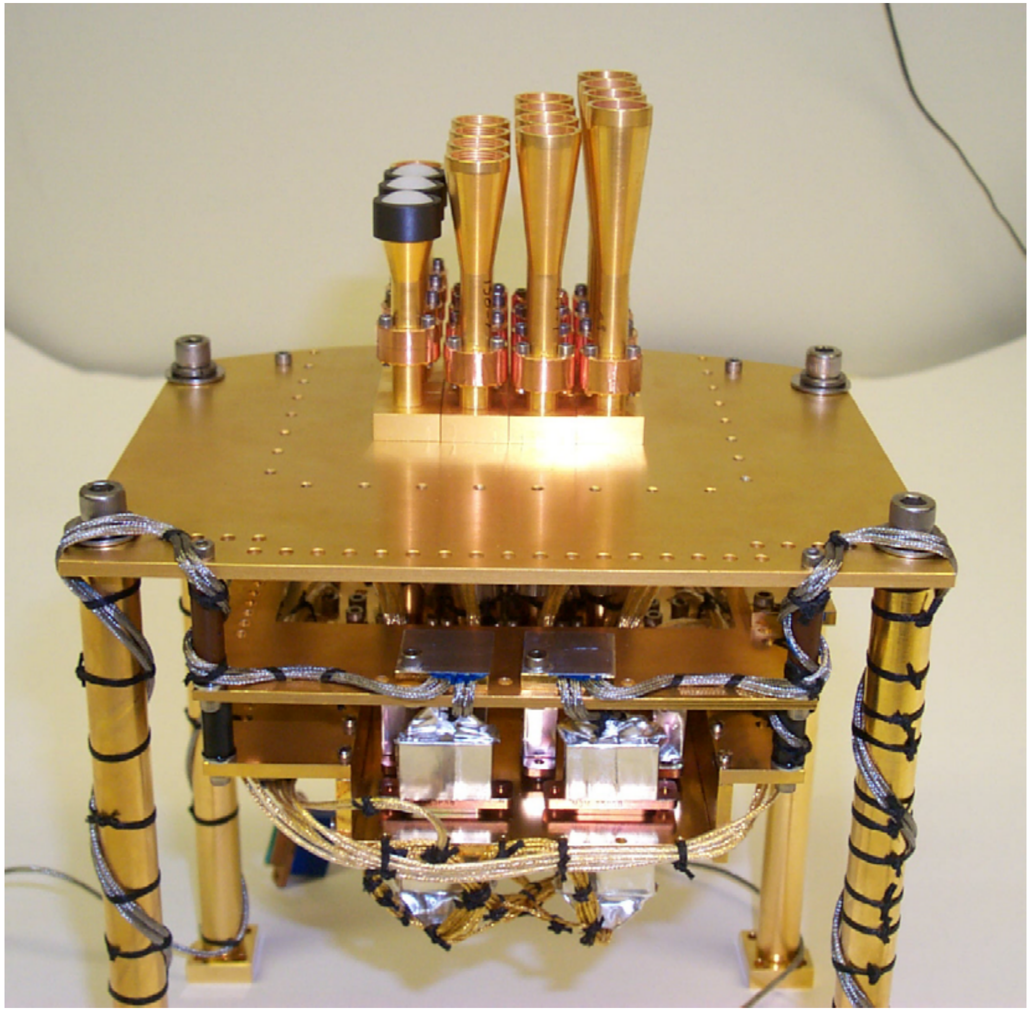

Layout of detector array and cryogenics

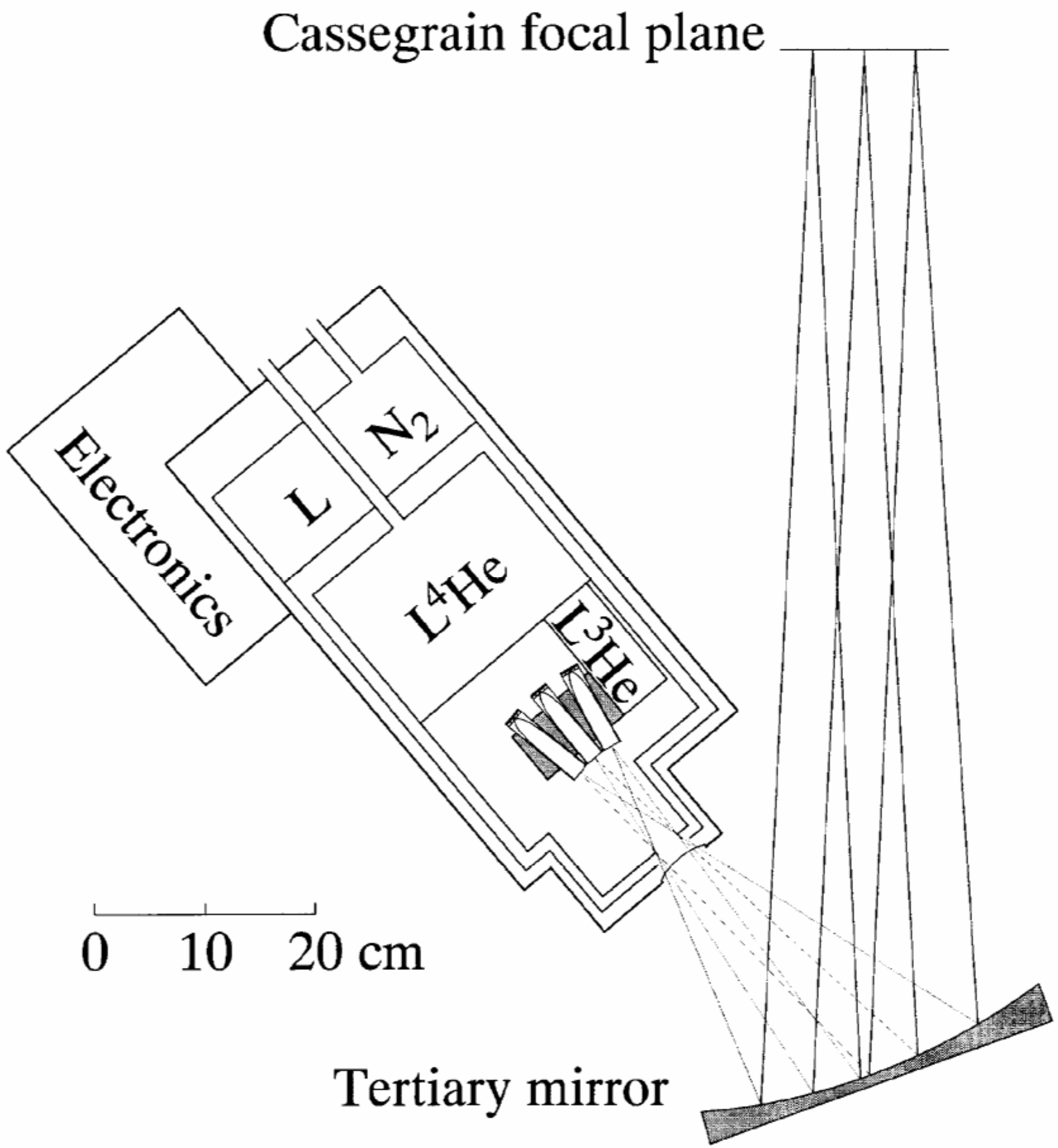

Balloon borne experiments

MAXIMA Gondola

Boomerang at the South Pole

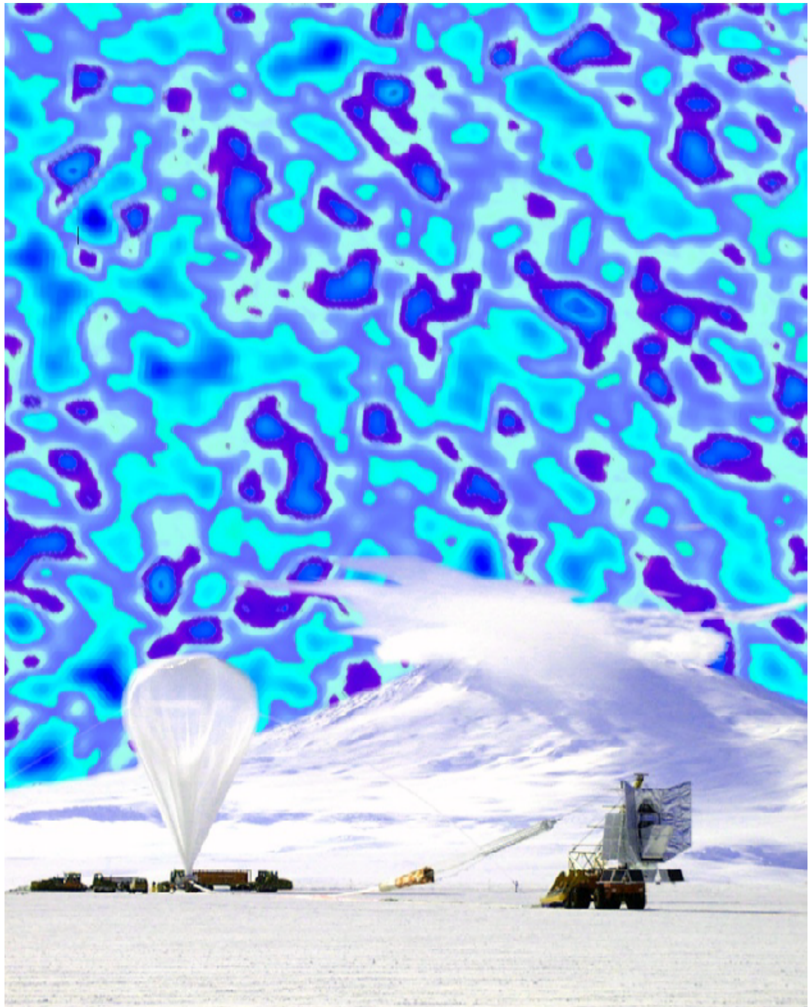

Measuring the CMB from Balloons

MAXIMA (P. Richards et al.)

Balloon-based experiment (launched in Texas)

Measure angular distribution of
temperature variations

Gondola prior to launch

Measurements at ~40 km altitude

Detector array in focal plane

Bolometers absorb radiation directly and translate temperature rise into electrical signal.

Array of 16 horn antennas coupled to individual bolometers at 100 mK.

Angular resolution: 10’ FWHM

Frequency bands: 150, 240 and 410 GHz
(~30 – 60 GHz BW)

Sensitivity: ~100 mK/$\sqrt{\mathrm{Hz}}$

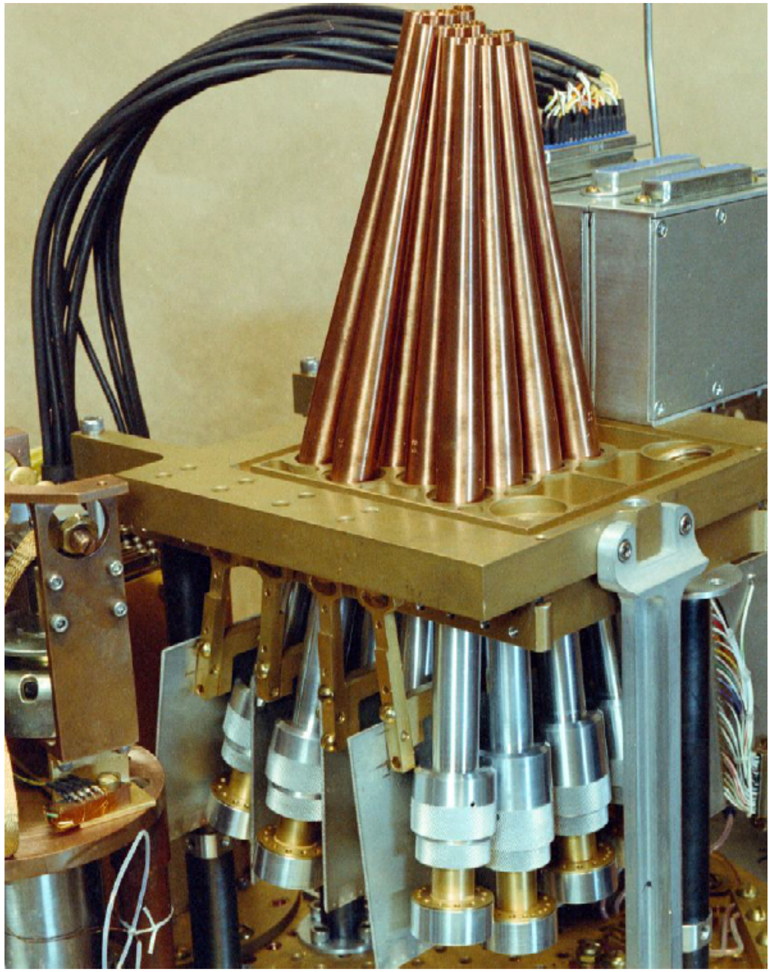

Sky map taken
by MAXIMA

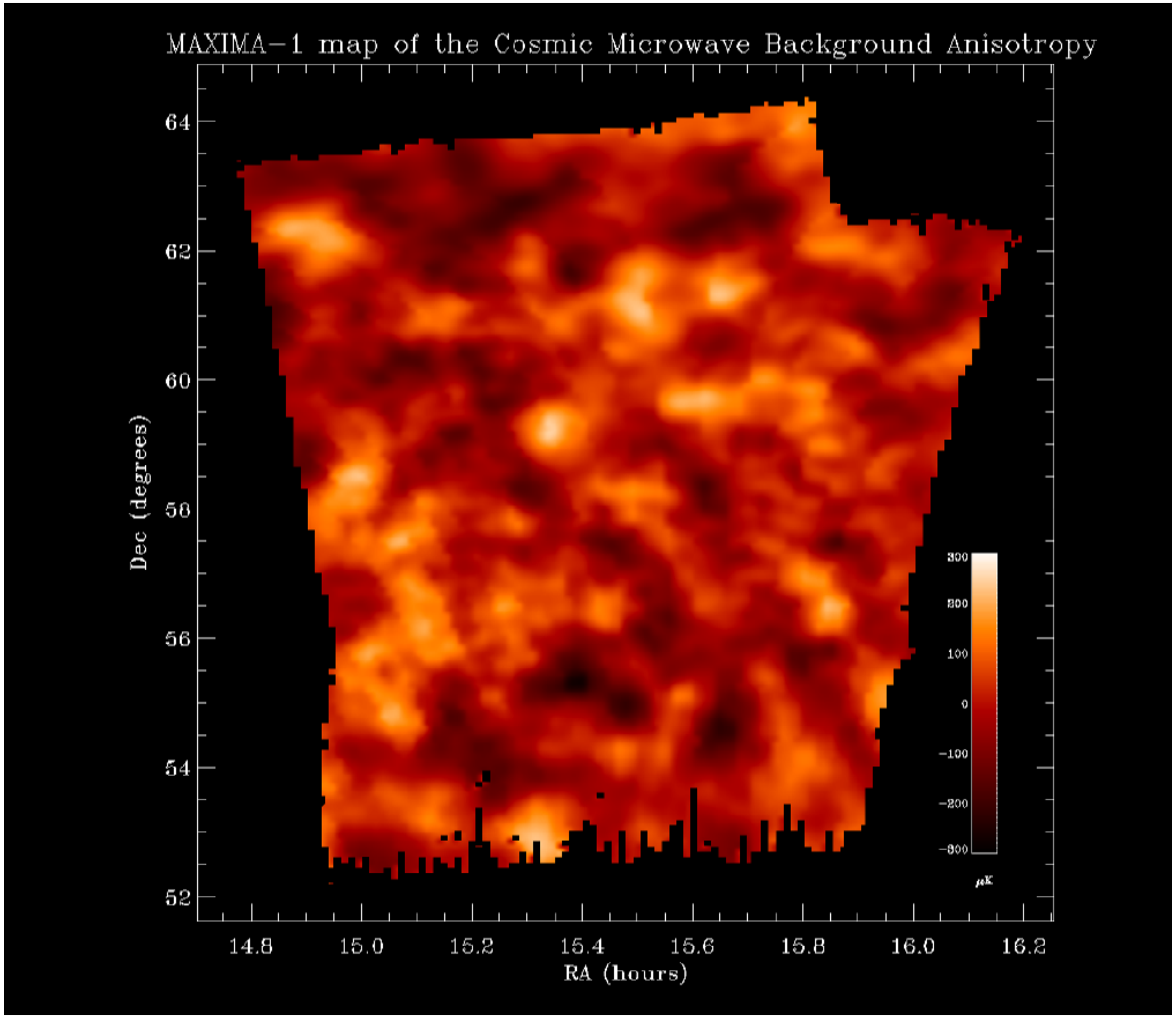

Observations in space: Wilkinson Microwave Anisotropy Probe (WMAP)

Launched June, 2002

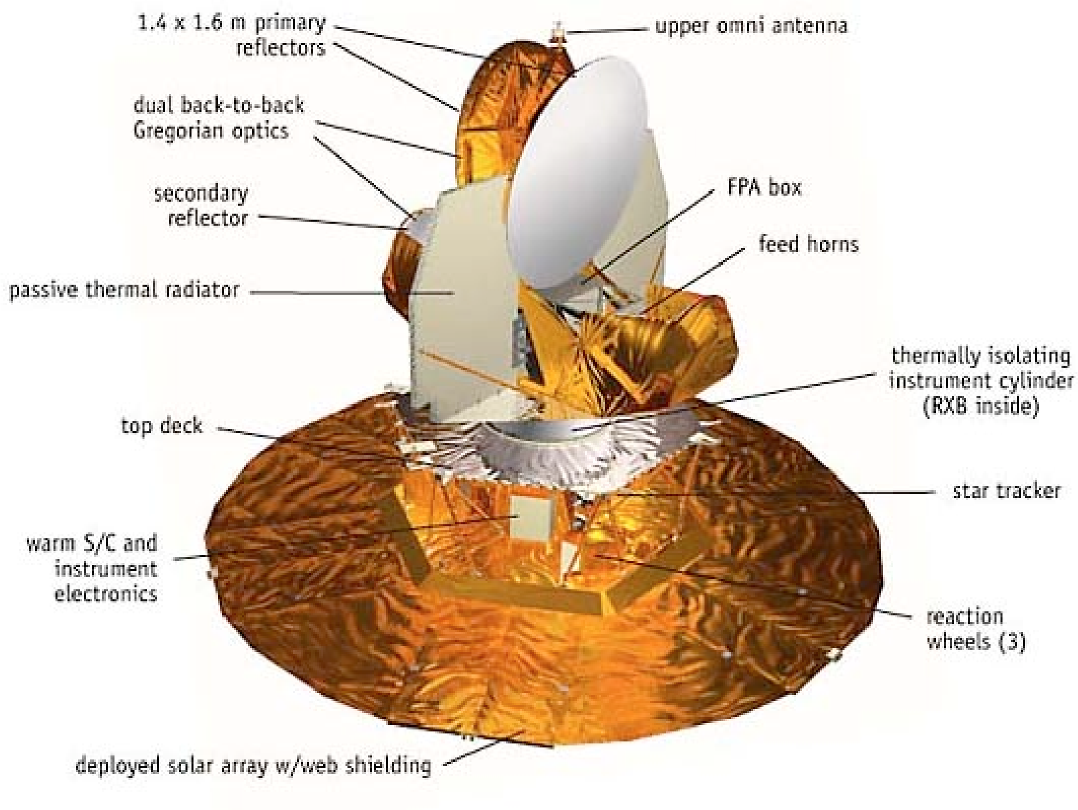

Most detailed CMB map to date

Eliminate atmospheric disturbances

Achieve full sky coverage

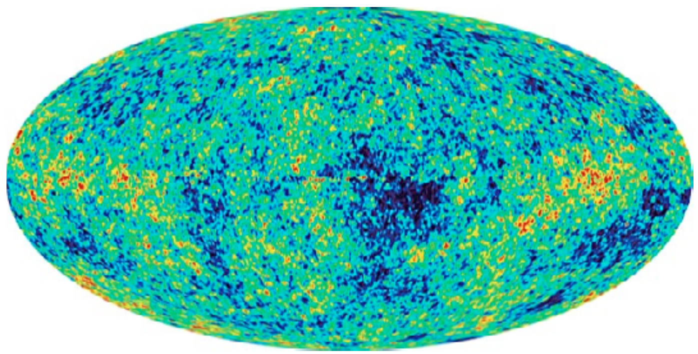

Some Next Generation Experiments

APEX-SZ	UCB, LBNL, MPIfR
South Pole Telescope	Univ. Chicago, UCB, LBNL, CWRU, CfA
PolarBear	UCB, LBNL, UCSD, McGill

Berkeley Group

William Holzapfel (UCB)
Adrian Lee (LBNL,UCB)
Paul Richards (UCB)
Helmuth Spieler (LBNL)

Martin White (LBNL,UCB) theory

John Clarke (LBNL,UCB) SQUIDs

Greg Engargiola (UCB RAL)
John Joseph (Eng. Div. LBNL)
Chinh Vu (Eng. Div. LBNL)

Brad Benford (UCB)
Sherry Cho (UCB)
Matt Dobbs (LBNL)
Nils Halverson (UCB – now Univ. Colorado)
Huan Tran (UCB)

+ 15 graduate students

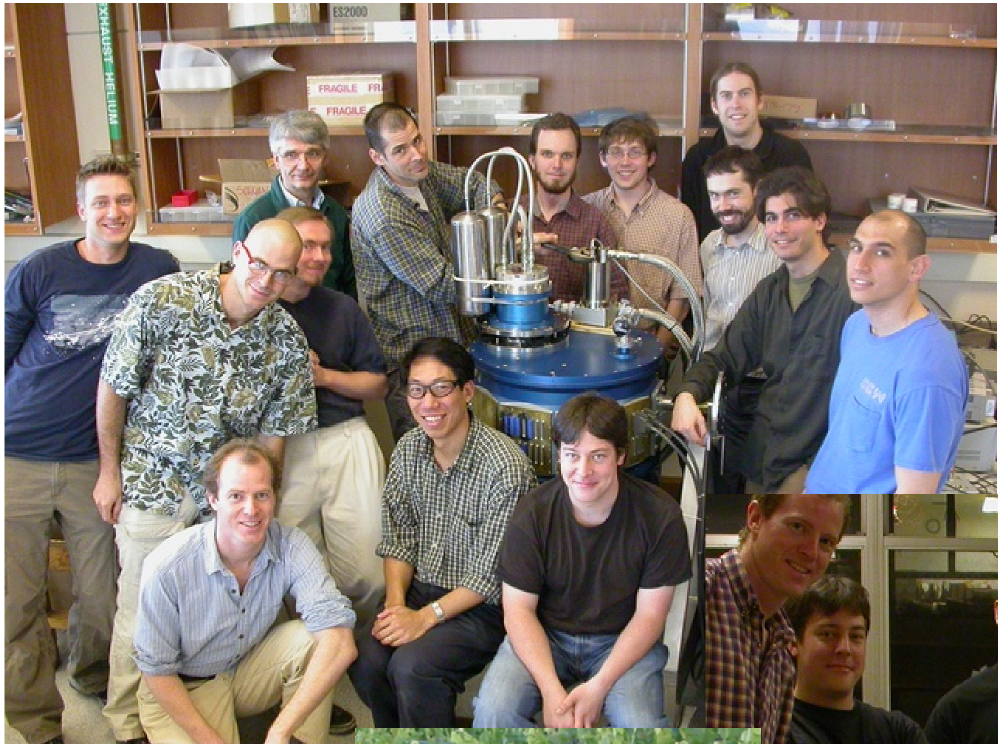

Some members of our group

First cool-down of APEX cryostat

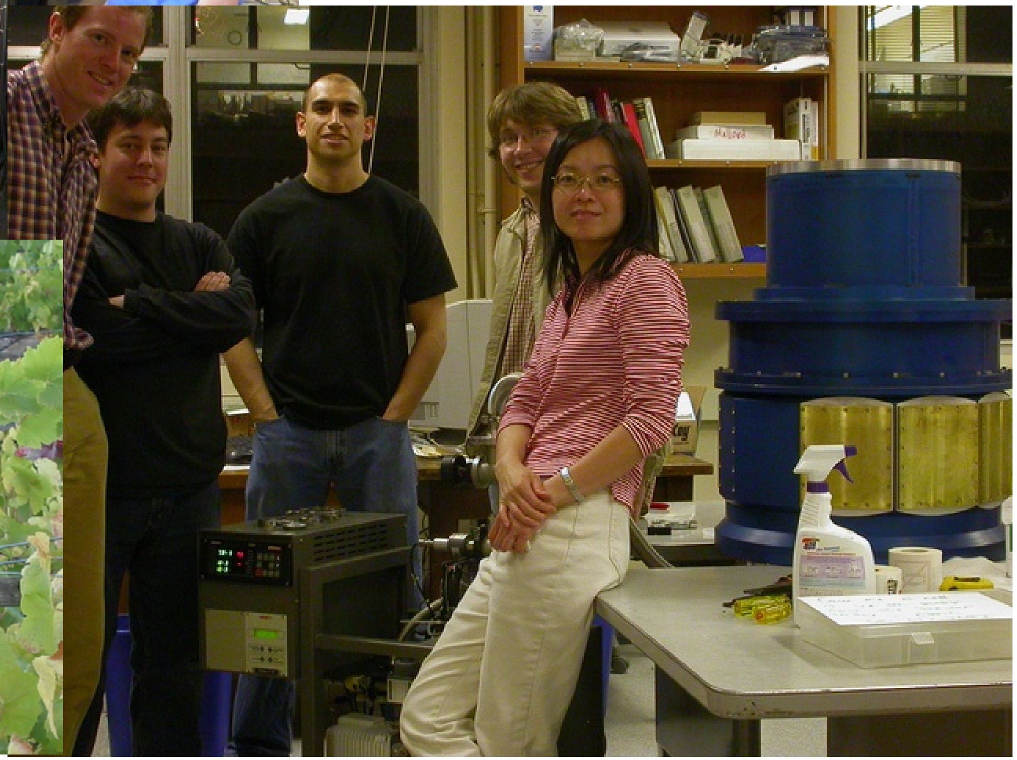

Paul Richards
in his
vineyard

APEX-SZ

Measure density of galaxy clusters vs. redshift (distance)

Cluster counts together with redshifts determine cluster dN/dz

constrain dark energy equation of state, w

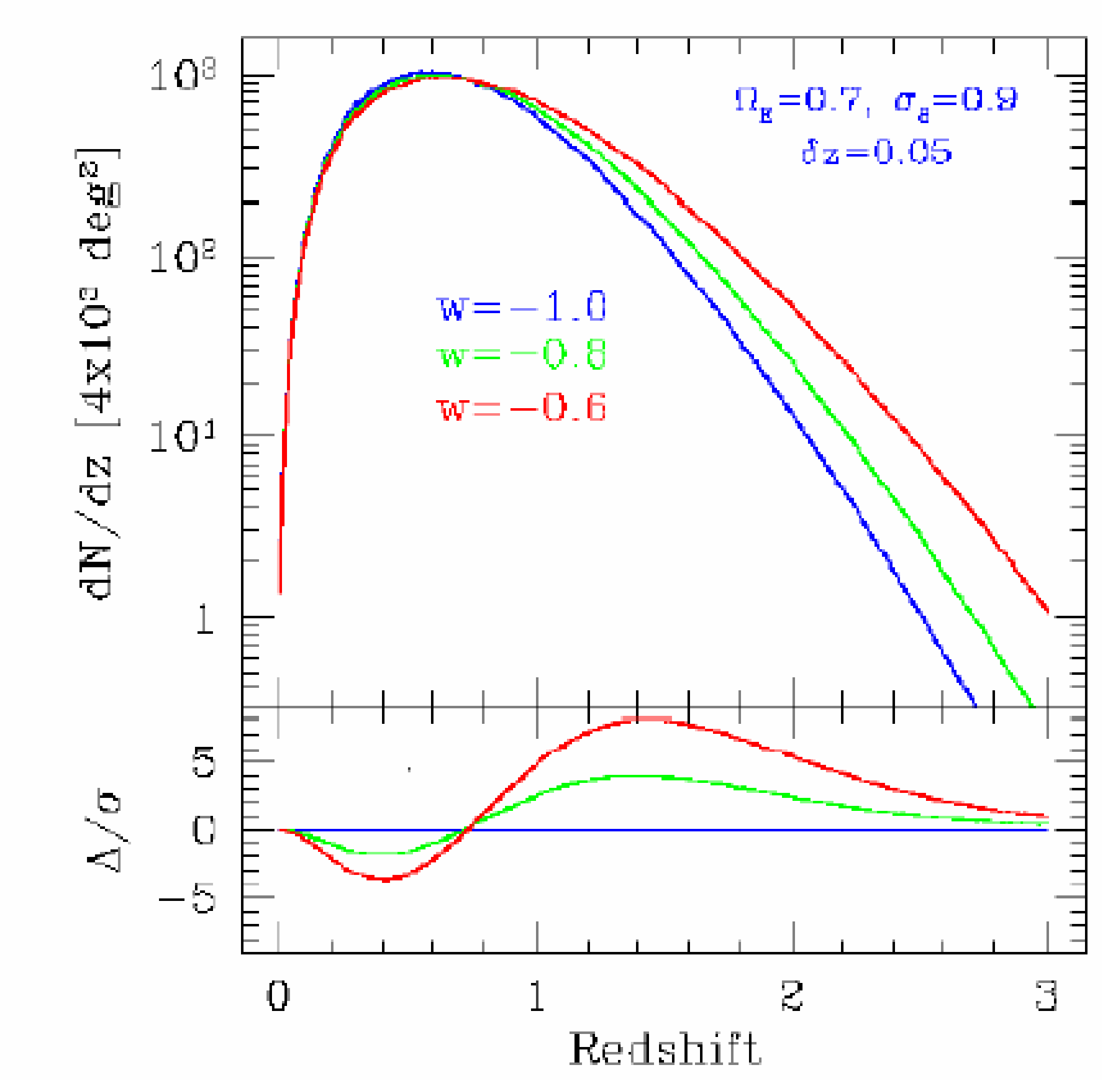

Growth of structure depends on cosmology:

Constrain matter density Ω_m

Complementary to DEEP & SNAP

different systematics

different correlations

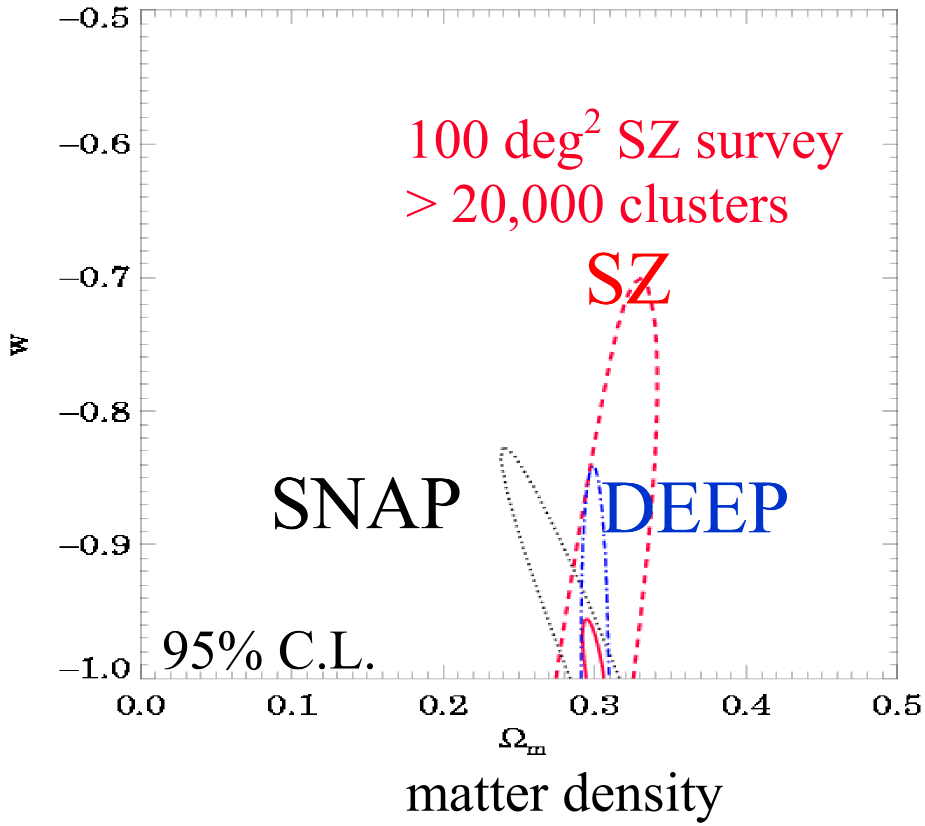

Measurement Technique: Sunyaev-Zel'dovich Effect

Inverse Compton scattering

Hot gas bound to clusters of galaxies scatters CMB

⇒ distorts black-body spectrum

⇒ measure motion of galaxies relative to CMB rest frame

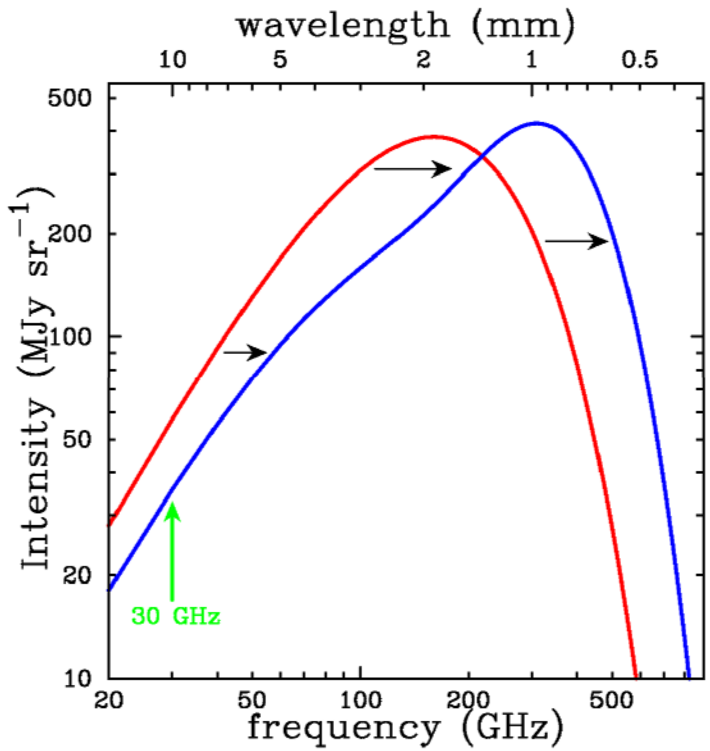

Difference between SZ and black body distributions

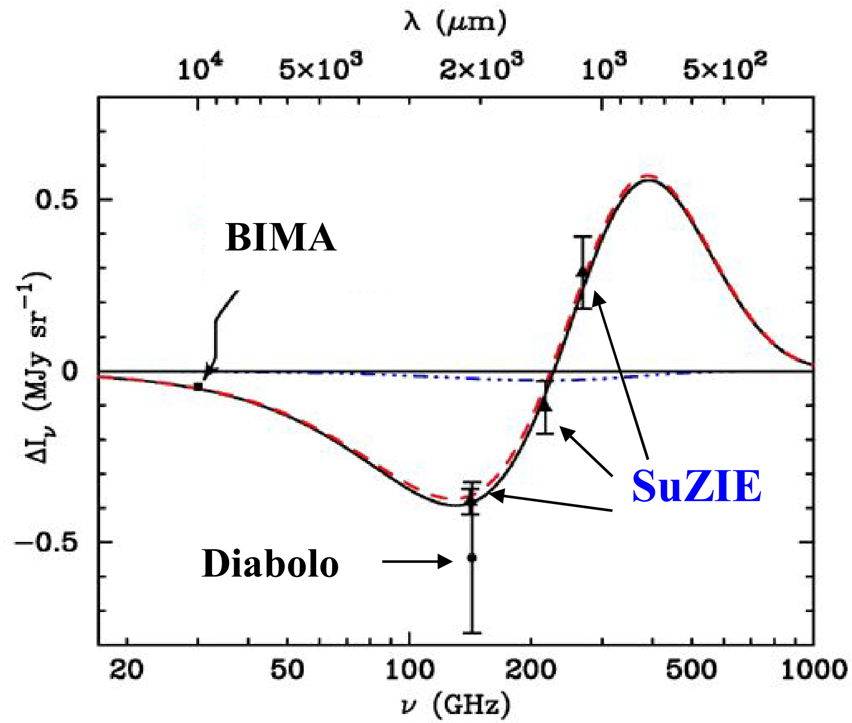

SZ effect independent of redshift

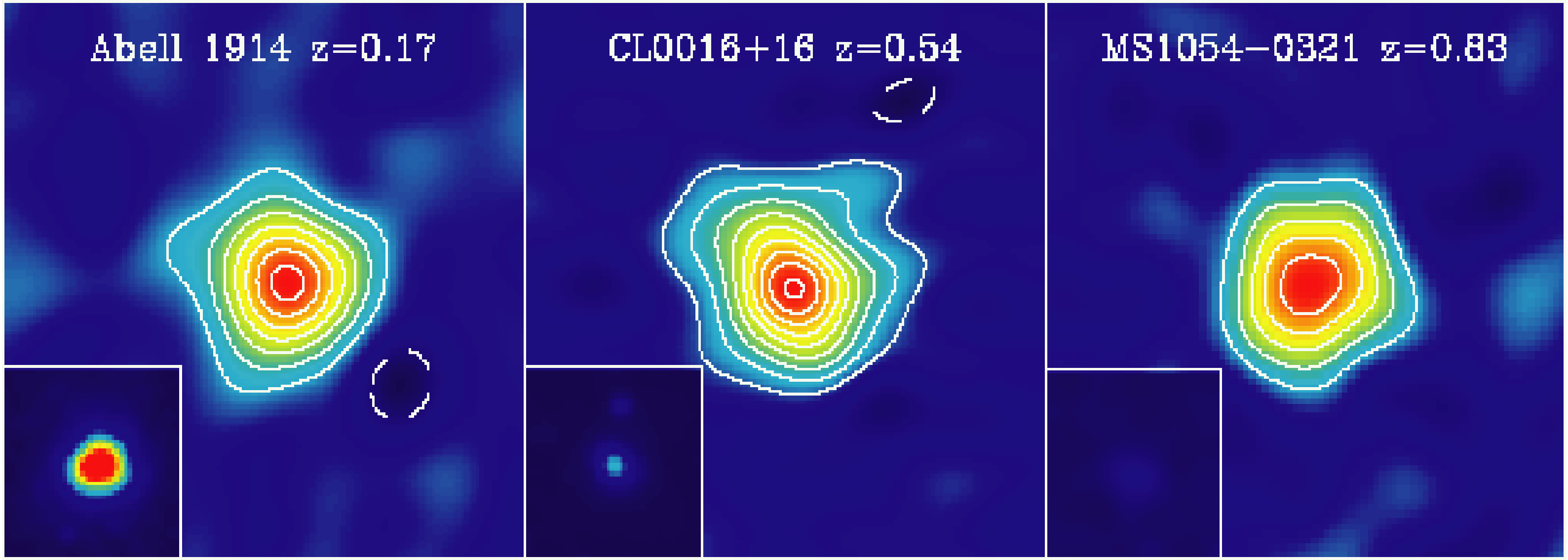

(Holzapfel et al.)

In contrast to x-rays (insets), SZ surface brightness is independent of redshift, so clusters can be seen at any distance.

However, x-ray data needed to determine temperature.

Emerging technique that requires greatly improved arrays.

Galaxy cluster searches

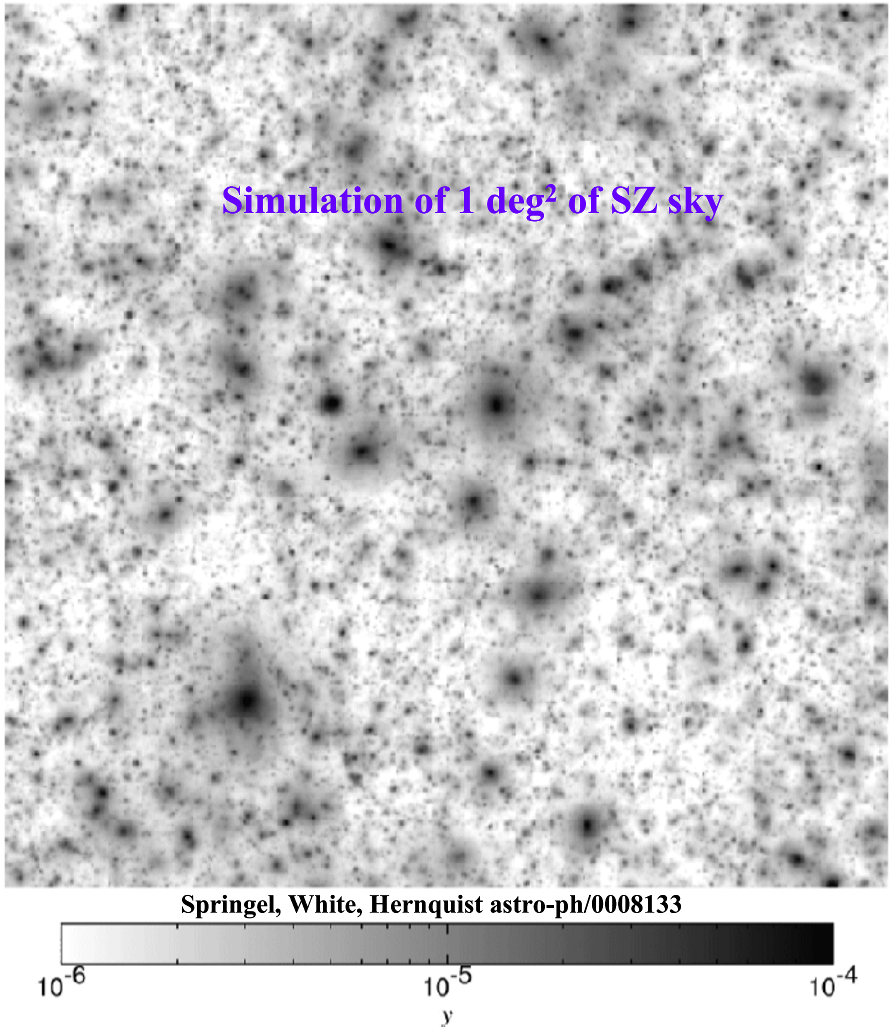

Springel, White, Hernquist astro-ph/0008133

Atacama Pathfinder Experiment (APEX)

Telescope

- Located at 5000m altitude in the Chilean Andes.
- 12m on-axis ALMA prototype
- 45” resolution at 150 GHz
- 30’ field-of-view
- Telescope operated by MPIfR/ESO/Onsala.
- Telescope installed in Chile

Berkeley SZ receiver

- 300 pixel focal plane array
- funded by NSF astronomy
- 25% of observing time
- First light Winter 2005

South Pole Telescope

- ~1000 pixel focal plane (multiplexed)
- 10m, off-axis design
- 1.3” resolution
- 1 deg. Field of view
- 100% time SZ observations
- Best mm-wave site
- First light 2007
- Funded by NSF Polar Programs (Univ. Chicago, Berkeley, Case Western, LBNL, SAO)

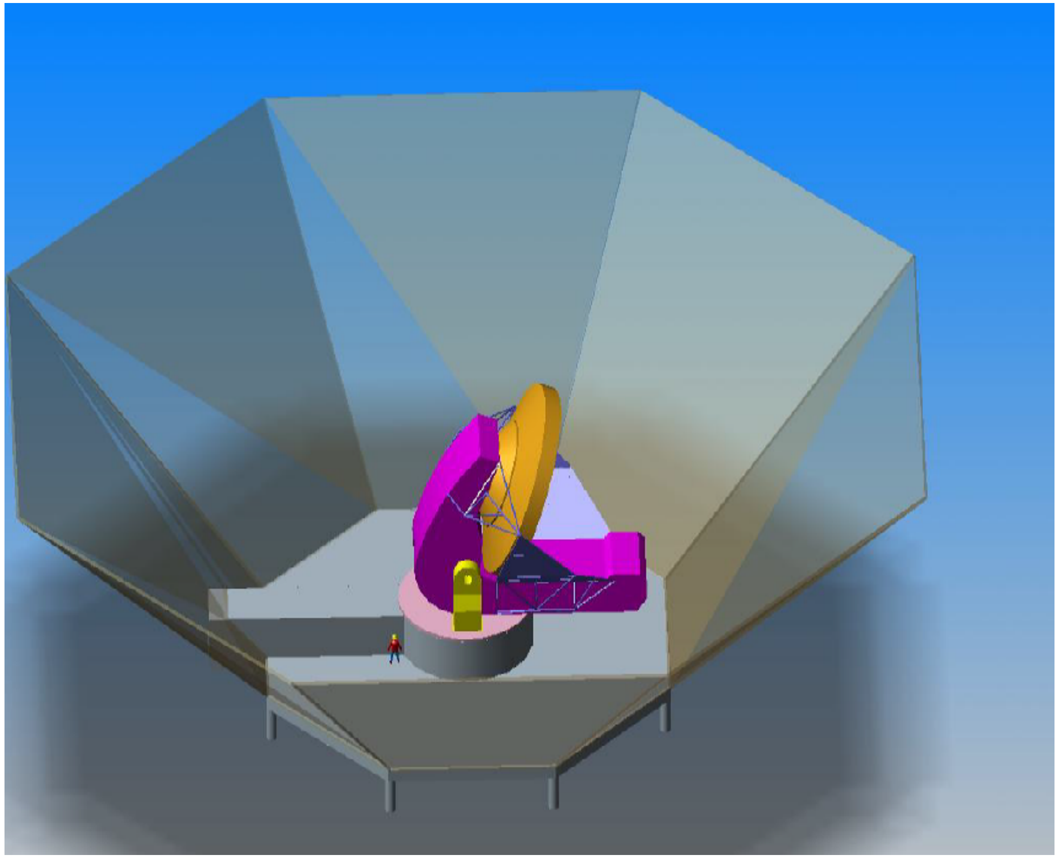

APEX and SPT are complementary:
APEX will be operational before SPT, but SPT will have ~5x faster cluster finding rate.

PolarBear

Polarization experiment: detect imprint of gravity waves from Big Bang
(“smoking gun” of inflation)

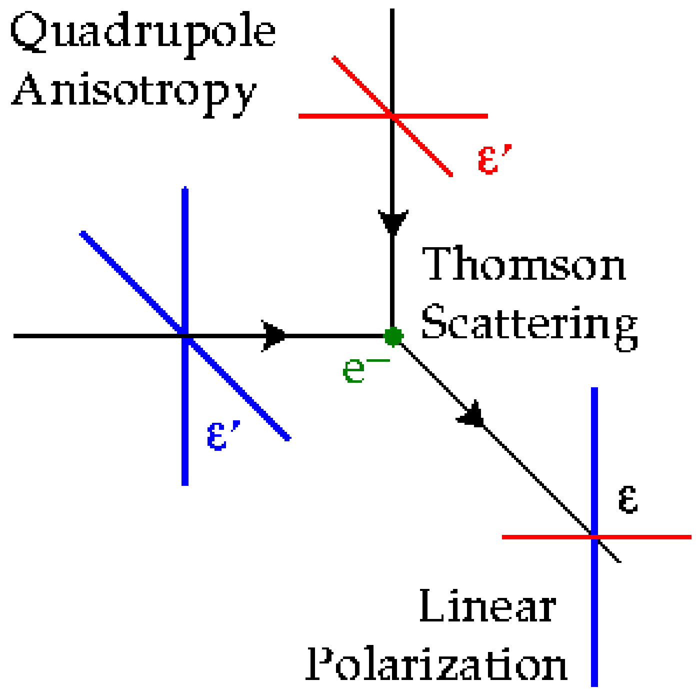

If CMB were perfectly isotropic, all polarizations would occur equally.

However, quadrupole anisotropy yields net polarization.

Gravity waves generate B-modes: Polarization field has net “handedness”.

E-modes

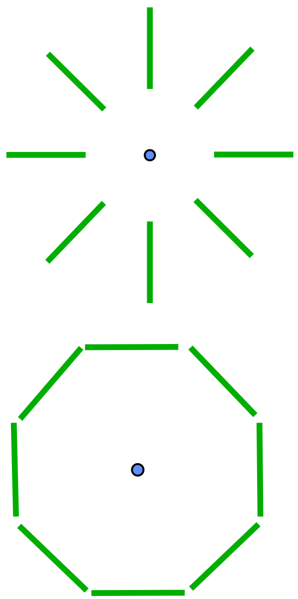

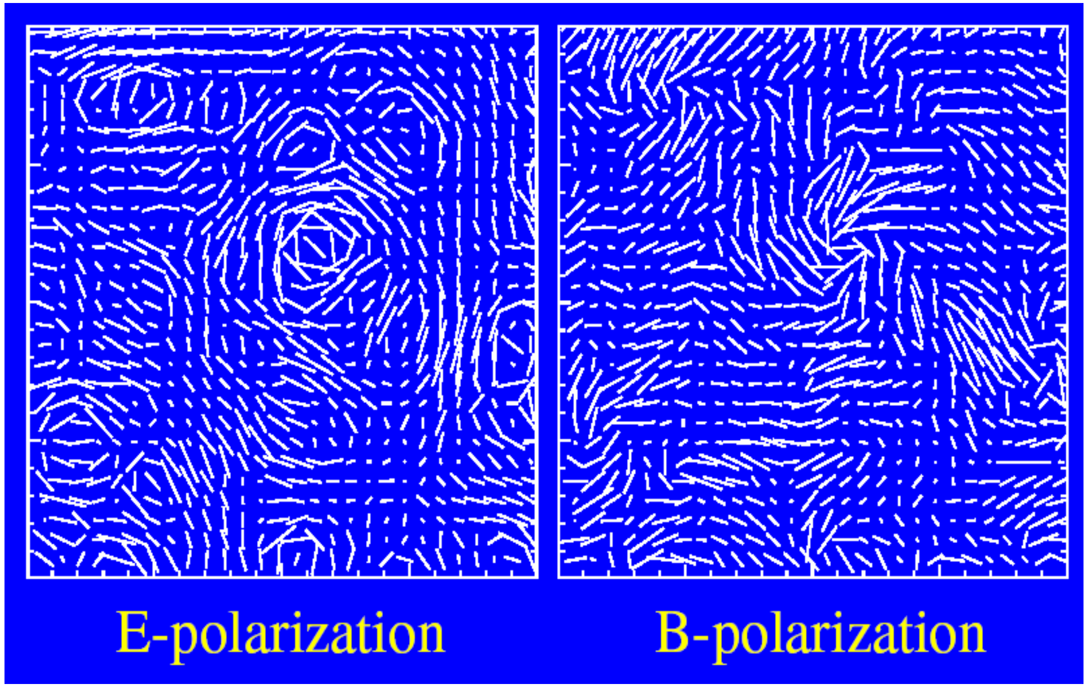

B-modes

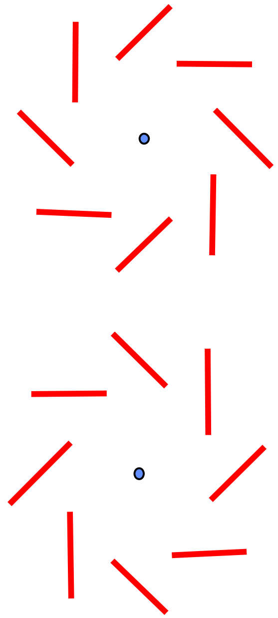

Wayne Hu

Density fluctuations give scalar perturbations $\Rightarrow$ E-modes
Gravity waves give tensor perturbations $\Rightarrow$ B-modes

E-mode polarization detected
(Carlstrom et al., DASI)

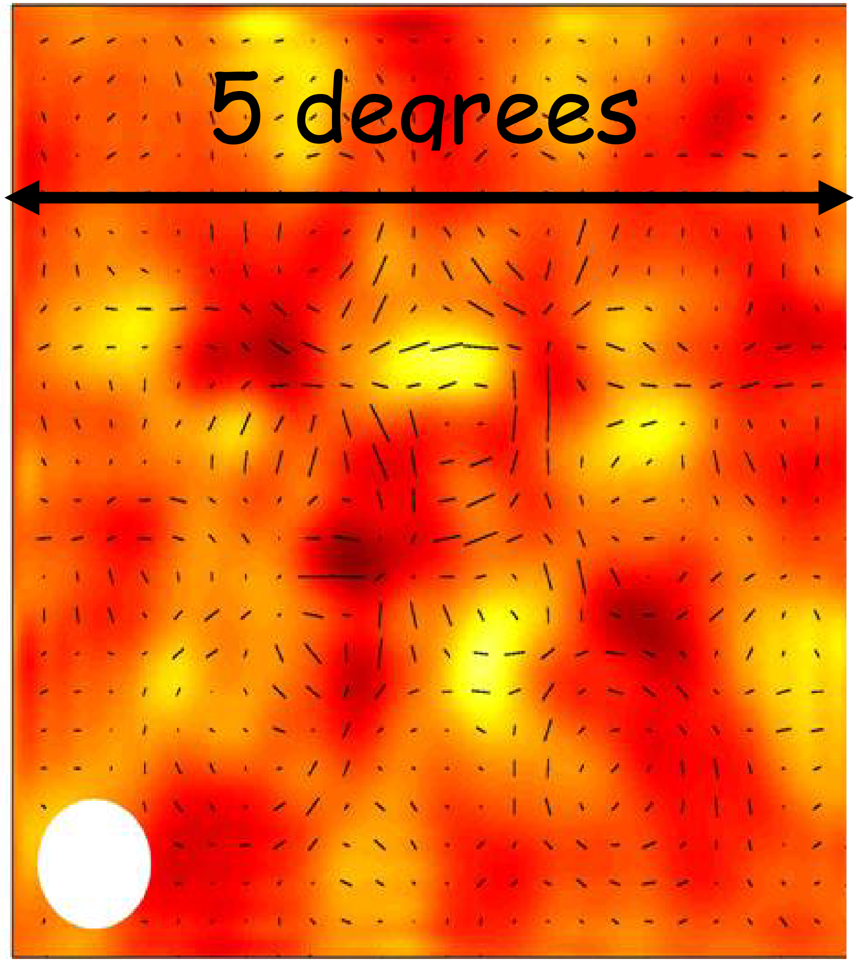

Challenge:

Detection and characterization of B-modes

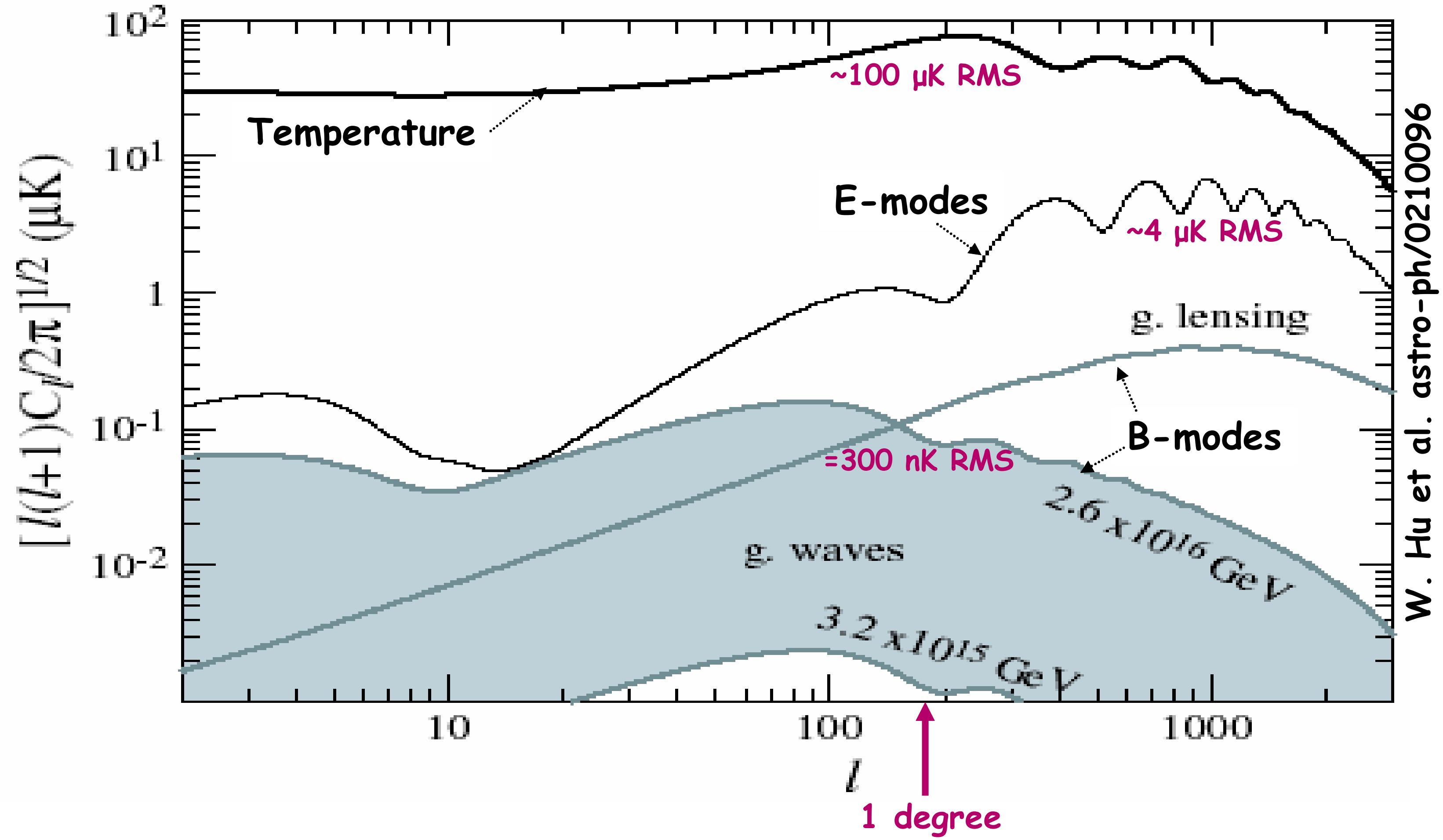

B-modes are also generated by weak lensing of E-mode polarization

Gravity wave signature and lensing have different angular scales

Requires 3m reflector to provide angular resolution.

Potential PolarBear Site: White Mountain, CA (~4000 m)

- atmospheric emission is nearly unpolarized.
- large sky coverage for primordial gravity waves
- sufficient resolution to measure and subtract out gravitational lensing signal.
- staged deployment – 300 elements, upgrade to ~3000 pixels
- multi-frequency polarization sensitive antenna coupled toTransition Edge Sensor bolometers
- testing facility for future satellite technologies, systematics, and foreground measurements
- first light 2007(?)

All of these experiments require a major step-up in sensitivity

Projected POLARBEAR Sensitivity

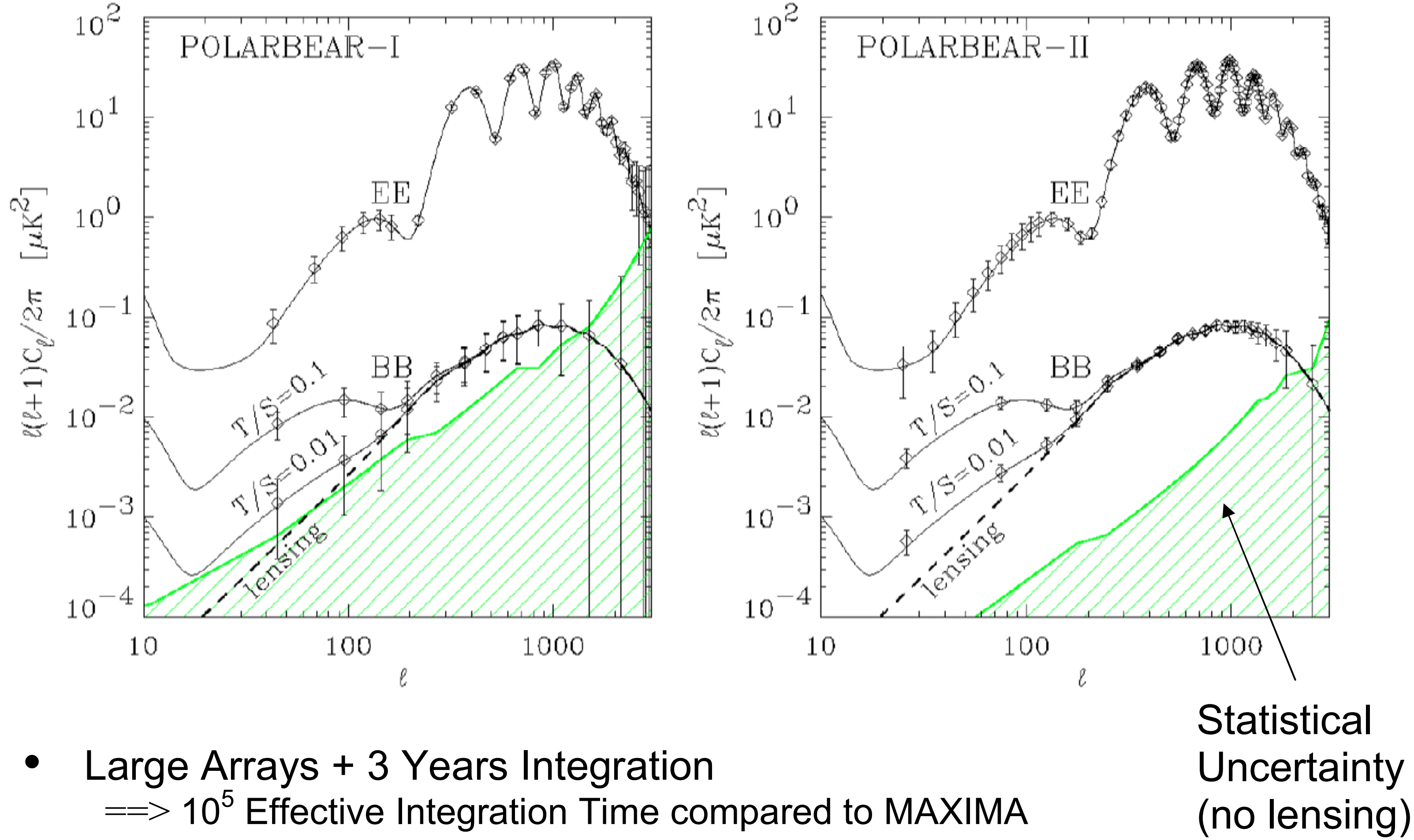

- Large Arrays + 3 Years Integration
  ==> 10^5 Effective Integration Time compared to MAXIMA
- Conservative Estimate using Achieved Sensitivity

Measurement Requirements

- 2.7 K black body spectrum: peaks at 150 GHz
- Antenna delivers power proportional to CMB temperature
- 2.7 K signal power: ~pW
- Next generation experiments aiming for 300 nK resolution
- Bolometers at photon shot noise limit
- 100 - 1000 increase in sensitivity needed
  - increase observing time $\Rightarrow$ ground-based experiments
  - large bolometer arrays

Thermal Detectors

Basic configuration:

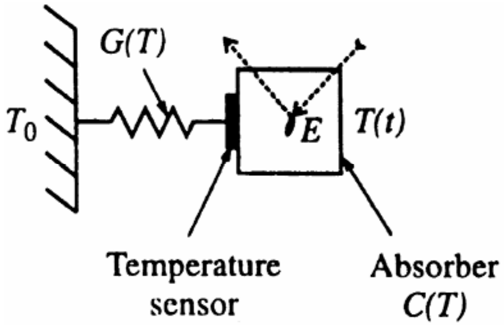

Assume thermal equilibrium:

If all absorbed energy E is converted into phonons, the temperature of the sample will increase by

$$\Delta T = \frac{E}{C}$$

where C the heat capacity of the sample (specific heat x mass).

At room temperature the specific heat of Si is 0.7 J/gK, so

E= 1 keV, m= 1 g $\Rightarrow$ ΔT= $2 \cdot 10^{-16}$ K,

which isn't practical.

What can be done?

a) reduce mass

b) lower temperature to reduce heat capacity
“freeze out” any electron contribution, so phonon excitation dominates.

Debye model of heat capacity: $C \propto \left(\frac{T}{\Theta} \right)^3$

Example: m = 15 μg

T = 0.1 K

Si $\Rightarrow$ C = 4·10^{-15} J/K

E = 1 keV $\Rightarrow$ ΔT = 0.04 K

How to measure the temperature rise?

Couple thermistor to sample and measure resistance change

Thermistors made of very pure semiconductors (Ge, Si) can exhibit responsivities of order 1 V/K, so a 40 mK change in temperature would yield a signal of 40 mV.

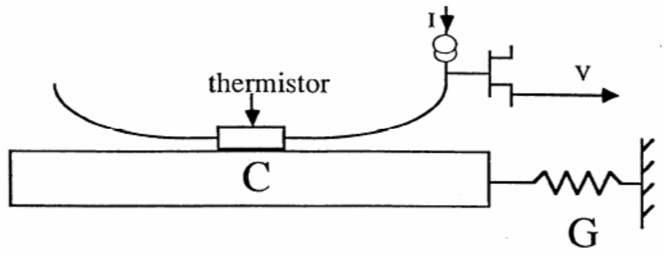

(Sadoulet, et al.)

Superconducting Transition Edge Sensors (TES)

Utilize abrupt change in resistance in transition from superconducting to normal state

The ultimate detection limit is determined by the thermodynamic noise of the sensor and the thermal noise associated with its resistance.

$$P_N = 4kT_S b + \sqrt{4kT_S^2 G b}$$

b = bandwidth

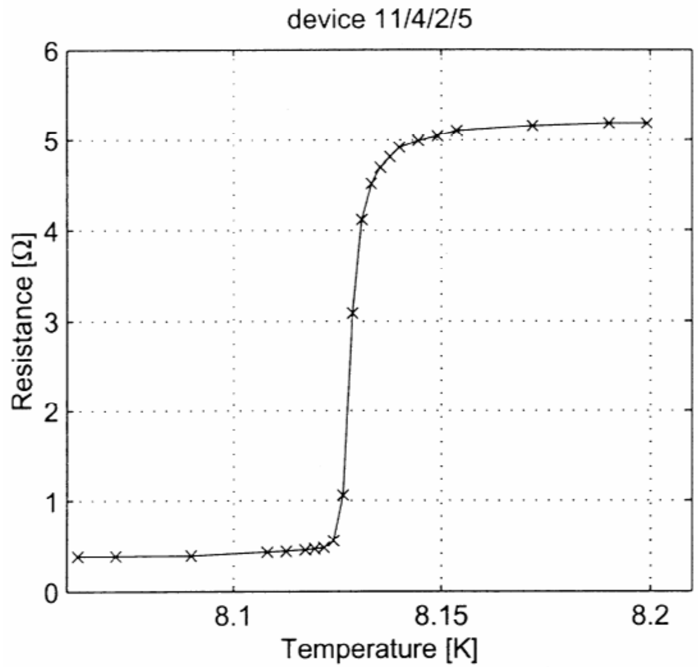

(Jan Gildemeister)

Worldwide activity on cryogenic detectors has led to impressive results, but devices have been

Hand-crafted

Critical to operate

⇒ only small arrays have been used

Recent developments have changed this picture:

1. Voltage-Biased Transition Edge Sensors

   ⇒ stable and predictable response

2. TES can be monolithically integrated using fabrication techniques developed for Si integrated circuits and micromachining.

   ⇒ fabricate large arrays with uniform characteristics

Transition temperature is adjusted by choice of thickness and materials in sensor sandwich:

1. Transition temperature depends on film thickness

2. Thin adjacent layers interact
   ("Proximity Effect")

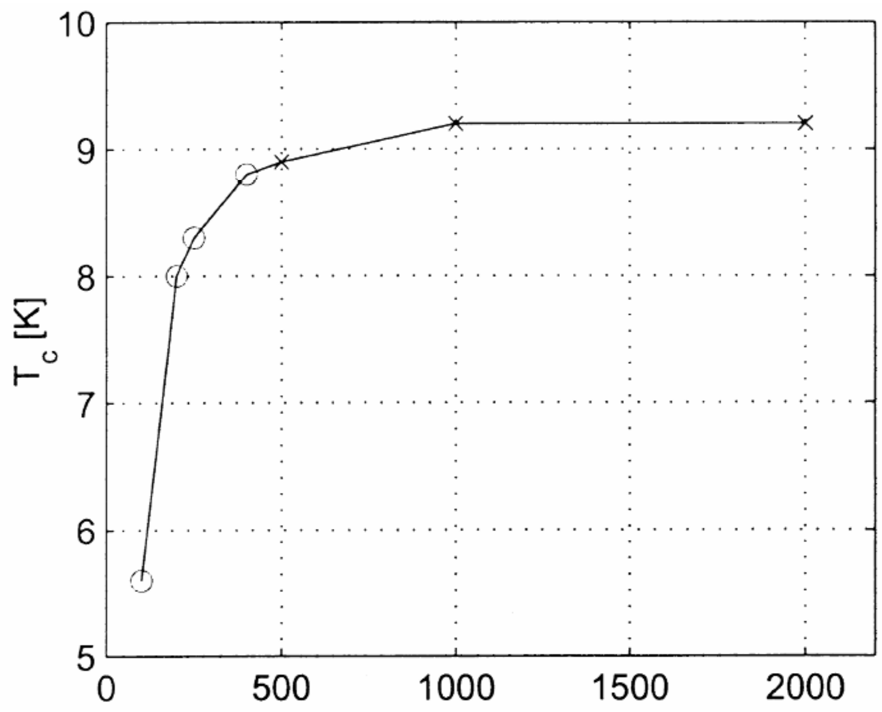

(Jan Gildemeister)

Voltage-Biased Transition-Edge Sensors

Required power is of order pW, i.e. voltage of order μV
current of order μA

Simplest to bias device with a constant current and measure change in voltage

Problem: power dissipated in sensor $P = I^2 R$

Increasing R $\Rightarrow$ Increasing P $\Rightarrow$ Increasing R $\Rightarrow$ Increasing P

$\Rightarrow$ thermal runaway

When biased with a constant voltage $P = \dfrac{V_b^2}{R}$

Increasing R $\Rightarrow$ Decreasing P $\Rightarrow$ Decreasing T $\Rightarrow$ Decreasing R

$\Rightarrow$ **negative feedback**

stabilizes operating point

In the transition regime the power is roughly independent of bias voltage.

Electrothermal negative feedback keeps total power in bolometer constant.

Change in power due to absorbed radiation must be balanced by change in bias power

$$Q_0 = -V \int_0^\infty I(t)dt$$

Signal current proportional to signal power.

⇒ calibration is determined only by magnitude of bias voltage.

Responsivity: $\Delta P = V_b \Delta I$

Noise spectral density:

$$i_n^2 = \frac{4kT_S}{R} + \frac{\sqrt{4kT_S^2 G}}{V_b}$$

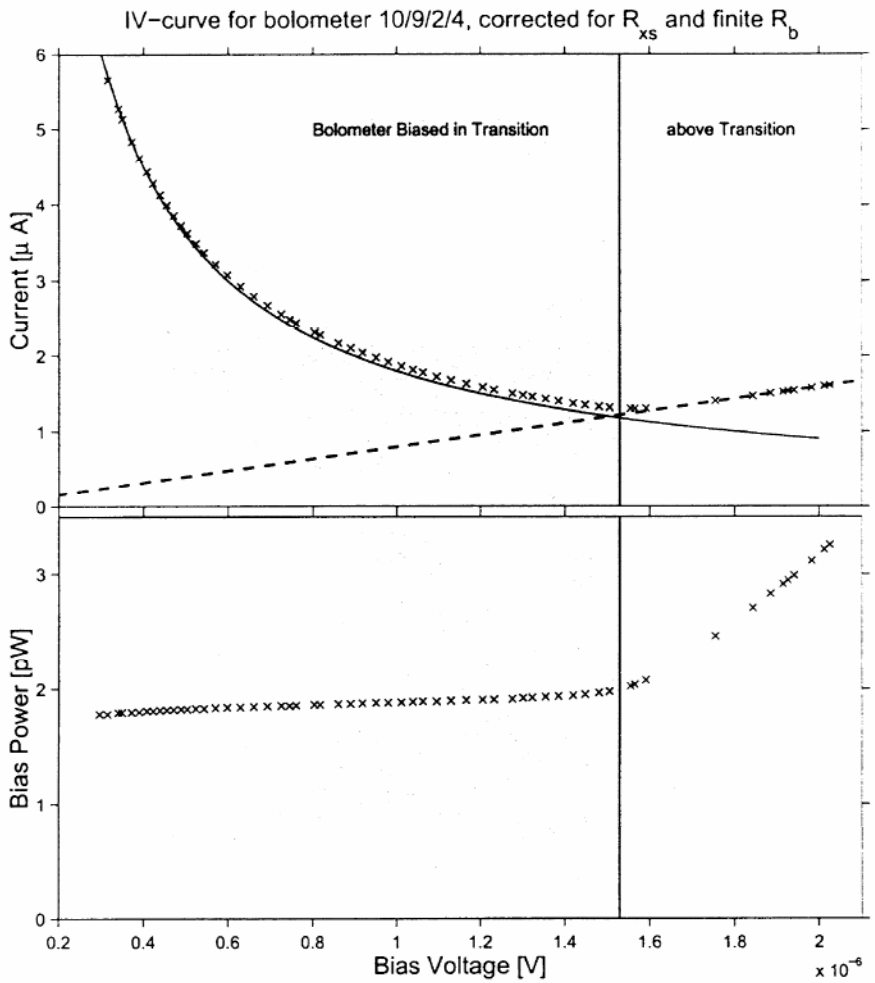

from Gildemeister

Important constraint:

Since sensor resistance of order 0.1 – 1 Ω, the total external resistance, i.e.

- Internal resistance of voltage source
- Input resistance of current measuring device

must be much smaller to maintain voltage-biased operation, i.e. < 0.01 – 0.1 Ω !

SQUIDs are good match for TES readout

- low temperature device
- very low noise possible
  (10 mK noise temperature compared to sensor temperature of 100 – 300 mK)
- low input impedance (input inductance ~100 pH)
- adequate gain to drive room-temperature amplifier without significant noise degradation

However,

- Input signal may not exceed 1/4 flux quantum (output periodic in Φ_0)
- Feedback loop required to lock flux at proper operating point (flux locked loop)

SQUIDs

Superconducting Quantum Interference Devices

Two Josephson junctions connected in parallel to form superconducting ring:

Two key ingredients:

1. Phase between two tunneling currents in Josephson junction is determined by current.

2. Magnetic flux in superconducting loop is quantized:

$$\Delta\Phi_0 = \frac{\pi\hbar c}{e} = 2.0678 \cdot 10^{-7} \text{ gauss cm}^2$$
$$= 2.0678 \cdot 10^{-15} \text{ Vs}$$

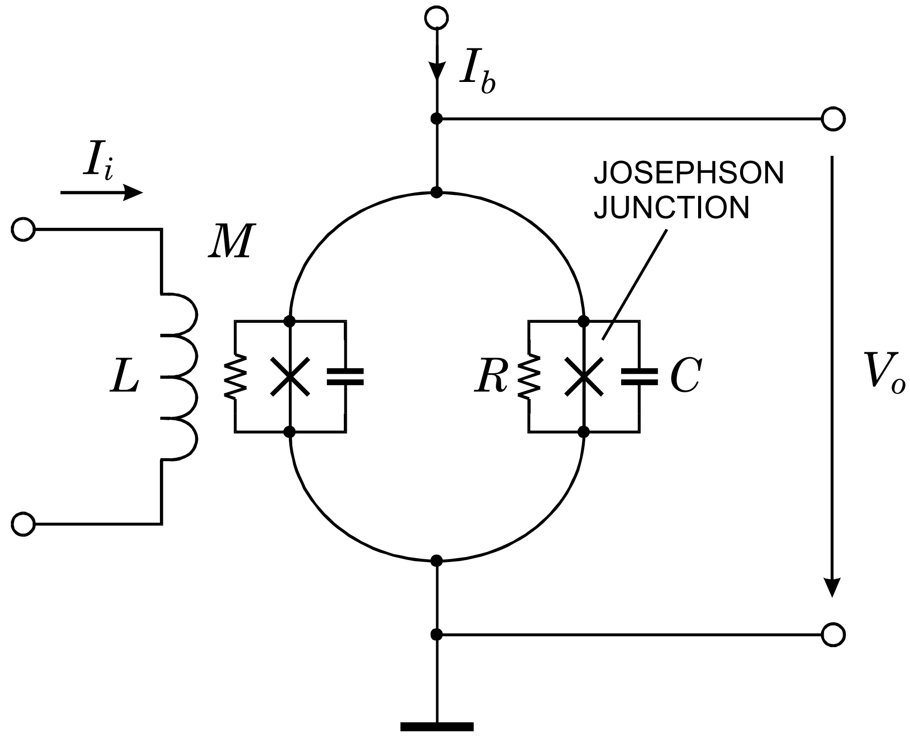

SQUID is biased by current I_b.

Input signal is magnetic flux due to current through coupling coil L.

Output is voltage V_o .

Current-Voltage Characteristics

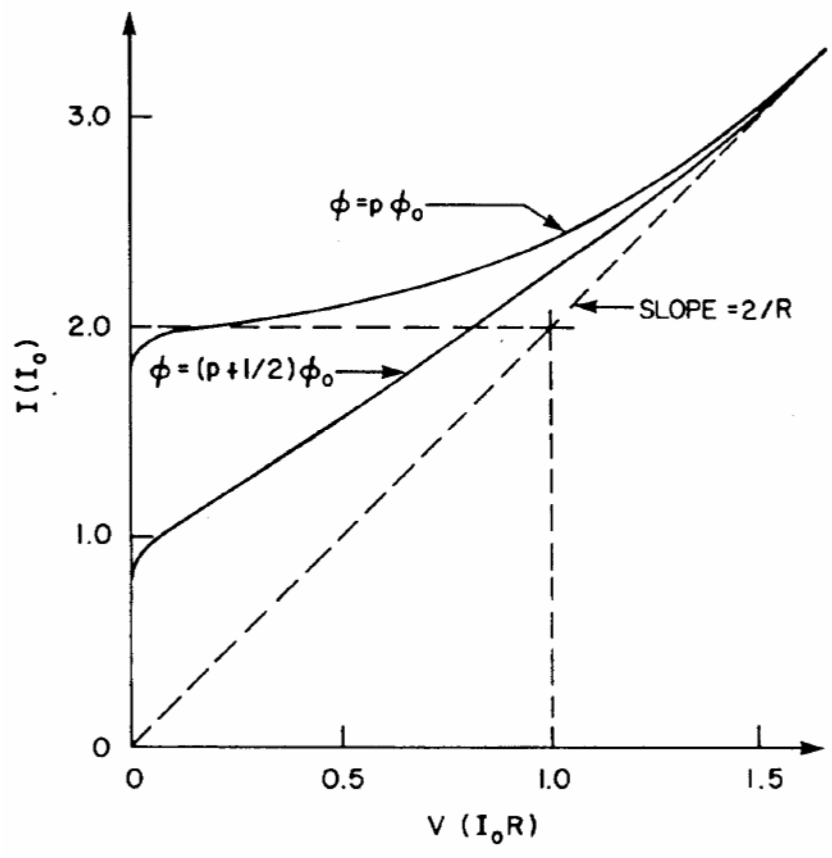

Output voltage V vs. flux Φ/Φ_0 as bias current I_B is increased

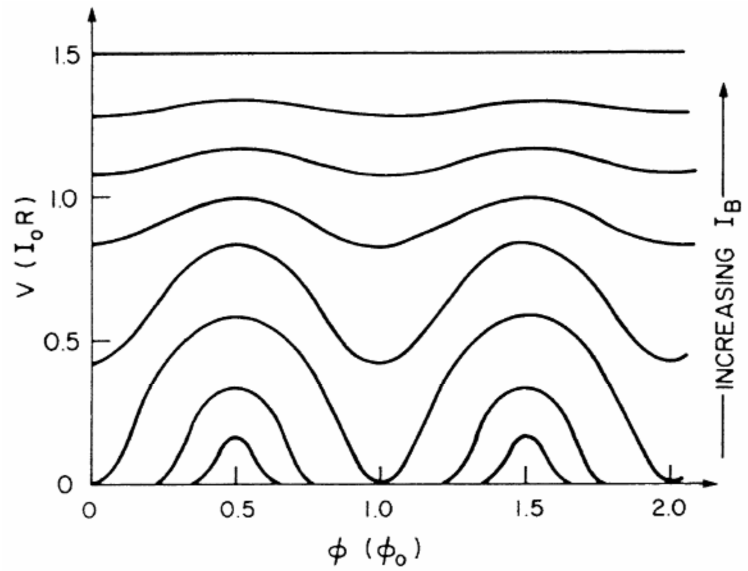

Flux sensitivity $V_\Phi \equiv \dfrac{dV_{out}}{d\Phi}$ at the operating point

However,

- Input signal may not exceed ¼ flux quantum
  (output periodic in Φ_0)

- Feedback loop required to lock flux at proper operating point (flux locked loop)

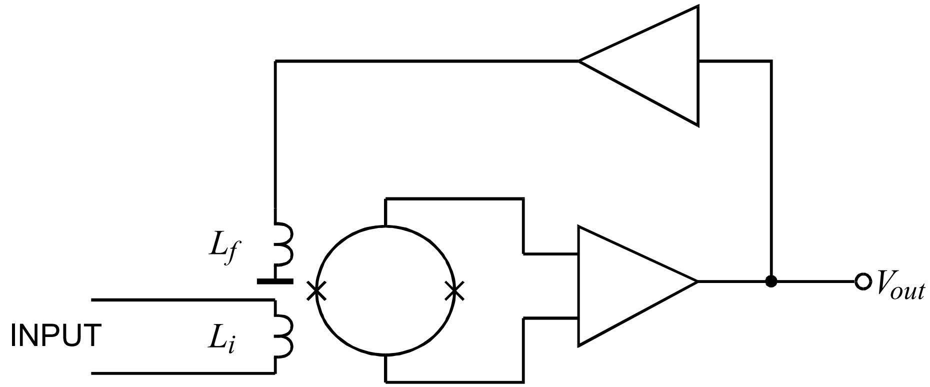

Feedback circuit limits frequency response.

H. Spieler, Frequency Domain Multiplexing for Large-Scale Bolometer Arrays, in Proceedings Far-IR, Sub-mm & mm Detector Technology Workshop, Wolf J., Farhoomand J. and McCreight C.R. (eds.), NASA/CP-211408, 2002 and LBNL-49993

Typical Parameters

Operating Temprature:	0 – 5 K (also high T_C SQUIDs)
Flux Sensitivity:	V_Φ =150 μV/Φ_0
Flux Noise:	1 to 10 $\mu\Phi_0$
SQUID Inductance:	100 – 500 pH
Input Inductance:	10 nH to 1 μH

Series SQUID Arrays

Array of SQUIDs with
input coils in series and
outputs connected in series.

We use arrays of 100 series-connected SQUIDs (fabricated by NIST).

$$\text{Sensitivity:} \quad \frac{\text{output voltage}}{\text{input current}} = M_i \frac{dV}{d\Phi} \approx 500$$

TES spiderweb

Need capture area comparable to wavelength

TES should be small for low noise

Mount TES in “spiderweb” made of mm beams of Si-nitride

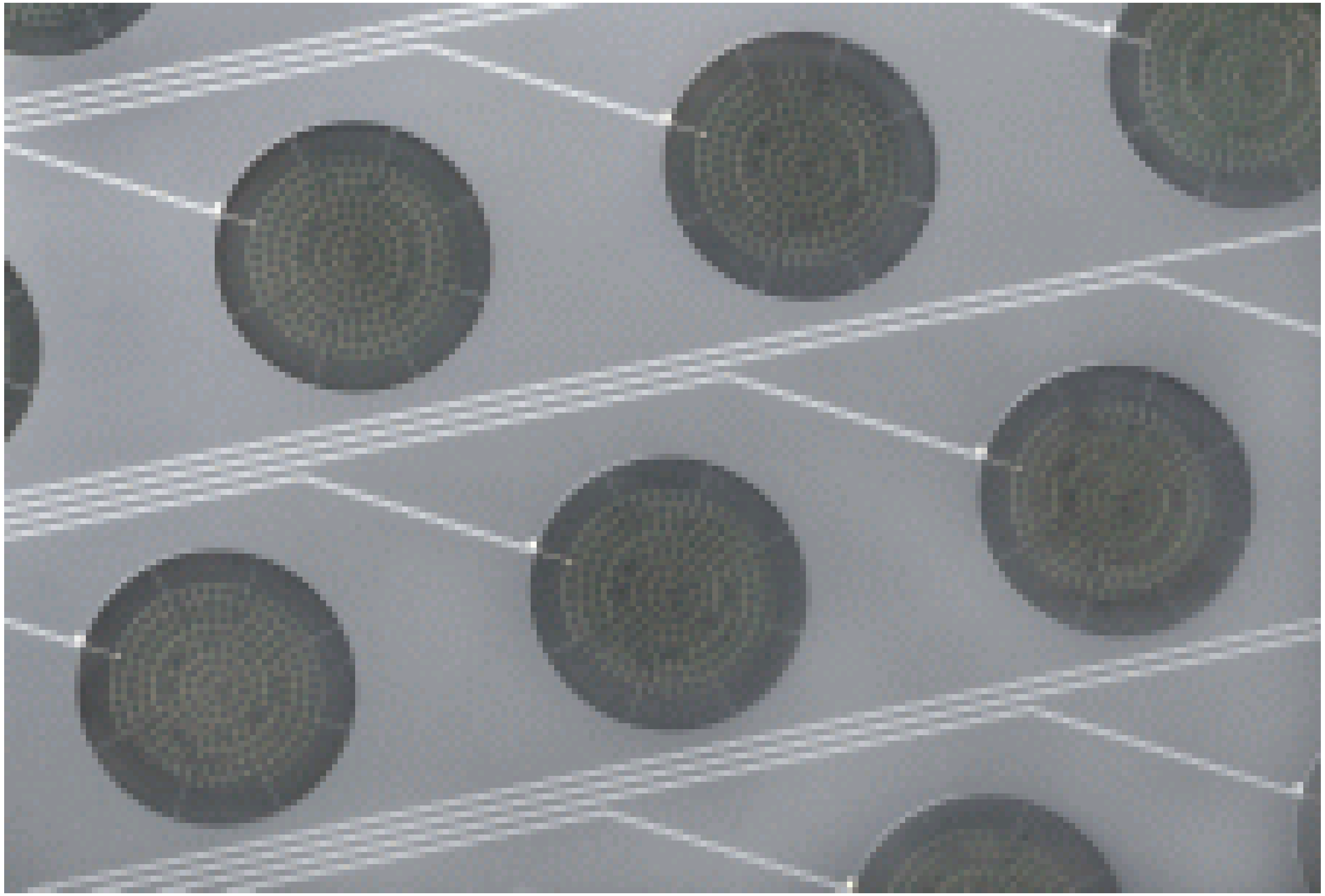

TES Spiderweb Arrays (APEX-SZ, SPT)

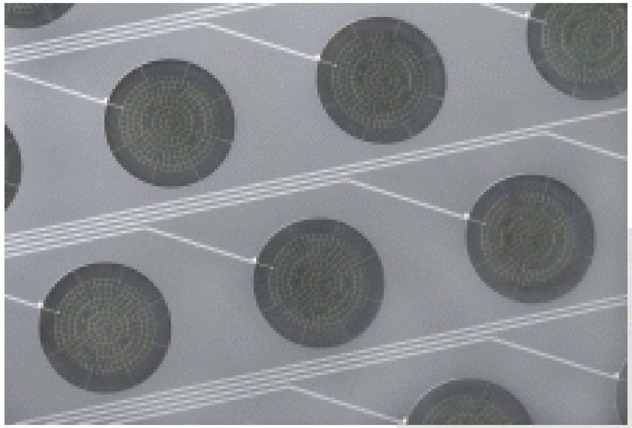

fabricated 55-bolometer array
(Jared Mehl et al.)

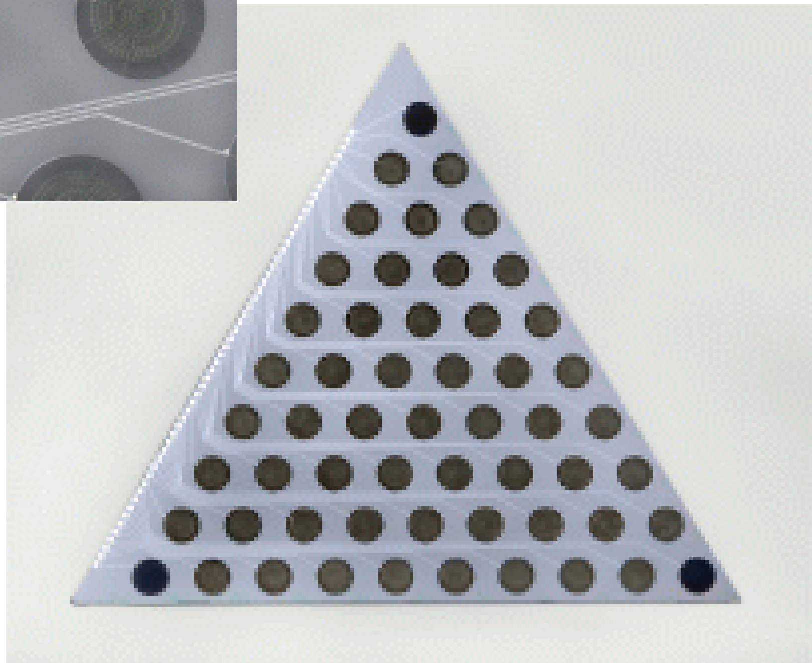

photomontage
of focal plane:

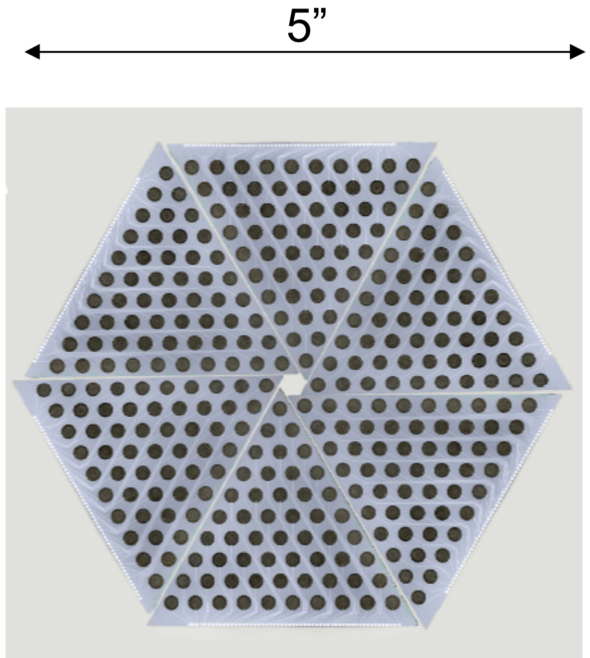

Cross-Section of a Pixel

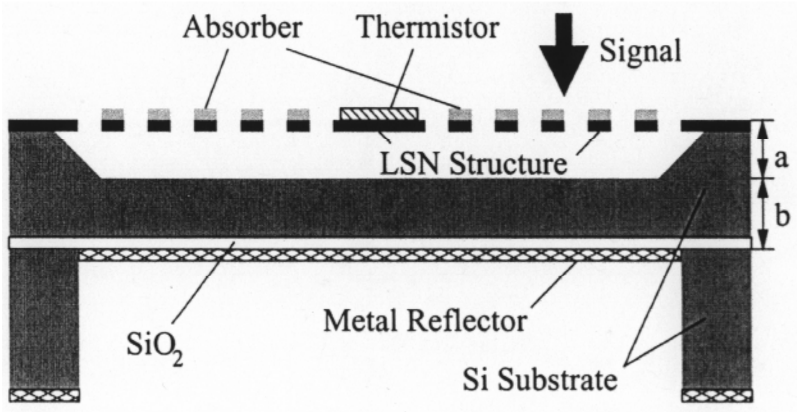

Wafers thinned to 150 μm have been run through fab

Calculated efficiency vs. backshort spacing

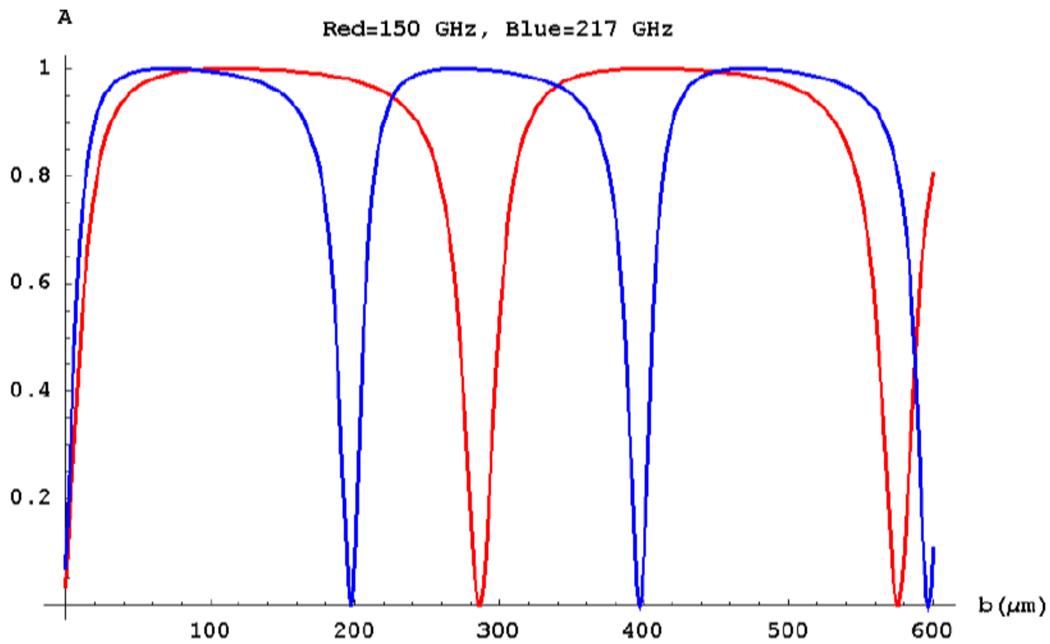

Backshort at a+b= 150 μm gives good efficiency at 150 and 217 GHz.

Focal Plane Design for APEX-SZ and SPT

Disk with machined conical horns positioned above bolometer arrray.

Horns match optics to bolometer plane.

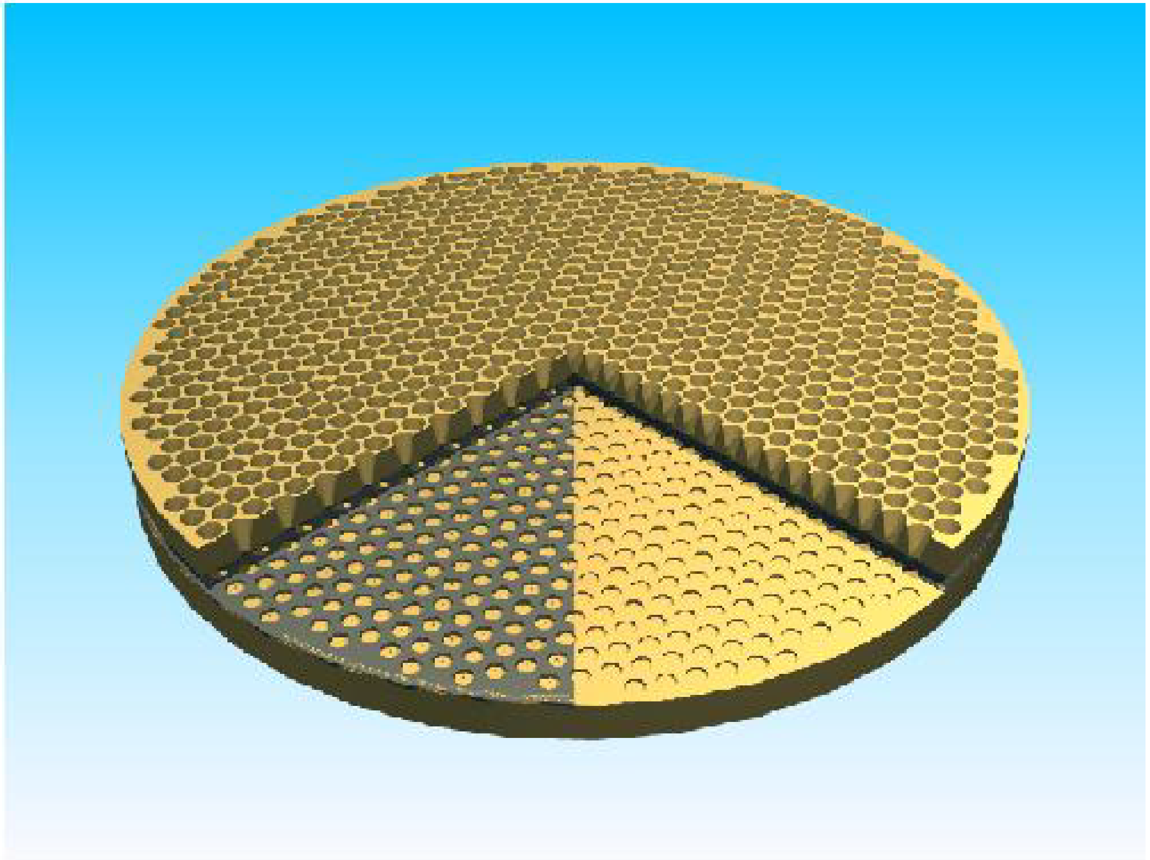

Antenna-Coupled Arrays

Highly integrated design

- Dipole antennas provides polarization sensitivity
- Phased dipole pair defines beam pattern
- On chip filters define frequency band
- Microstrip transmission lines transfer received power to load resistor coupled to bolometer
- Dual polarization in same pixel (duplicate circuit with antenna rotated
- Multiple frequencies possible

TES sensors multiplexed

Extensible to wideband polarization-sensitive antennas with multiband readout.

Antenna-Coupled Prototype Pixels (Mike Myers)

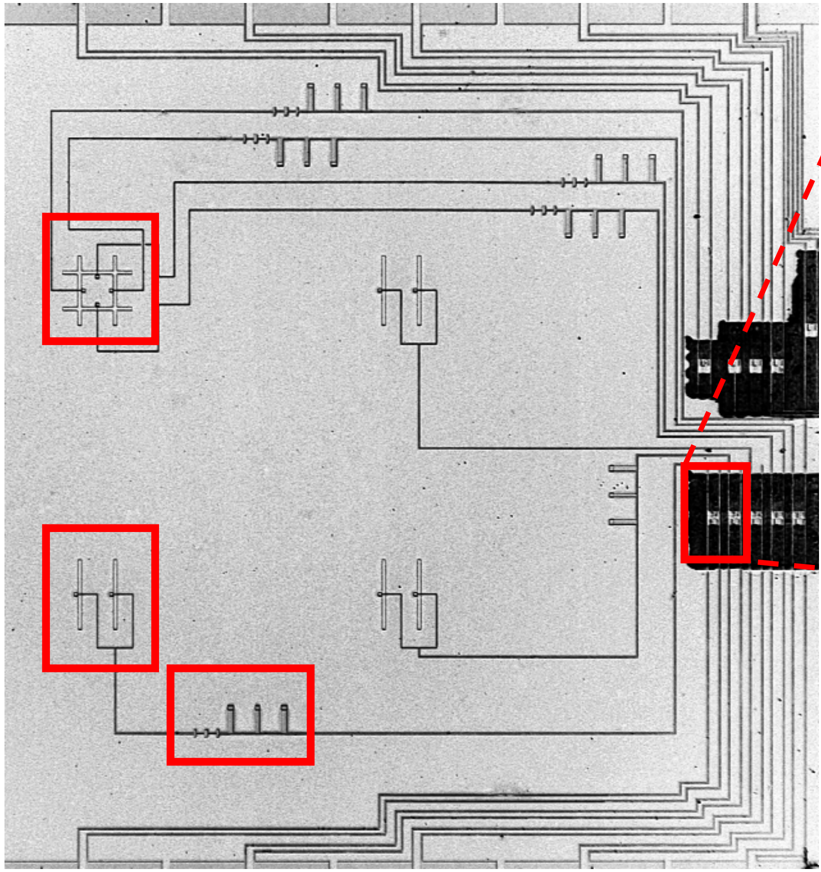

Dual pol. antenna at upper left
(after Chattopadhyay and Zmuidzinas)

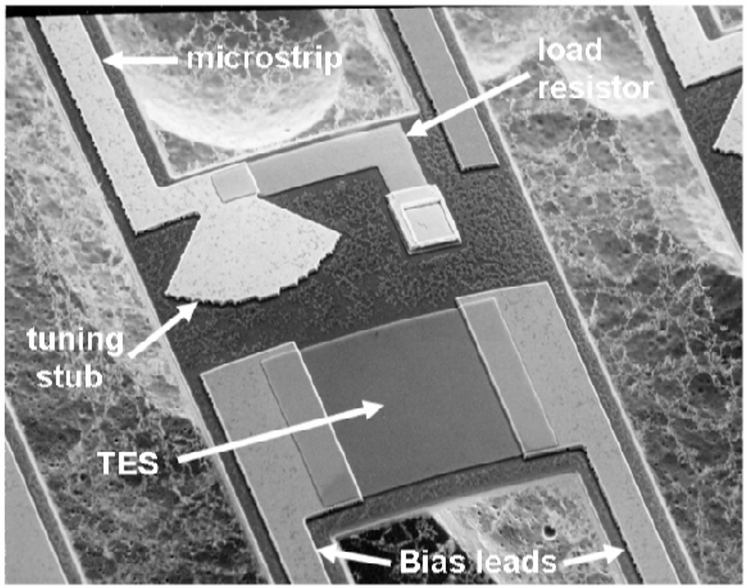

Microstrip fed double slot dipole antenna

Bandpass filter at 217GHz, 40% BW

Lowpass filter to remove spurious passbands

Microstrip terminated on a nitride suspension, power measured with TES

Antenna coupling to optics by dielectric lenses

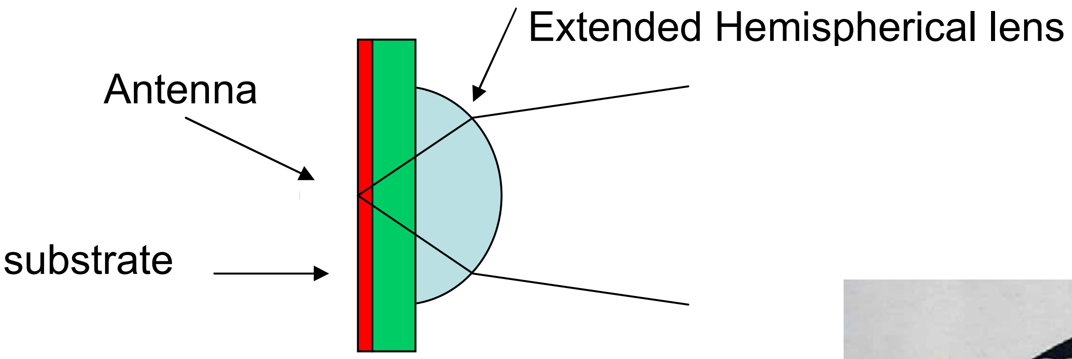

- Well developed (SIS mixers, etc.)
- High antenna gain, symmetric beam
- Forward radiation pattern
- Efficient coupling to telescope (Similar to scalar horn)

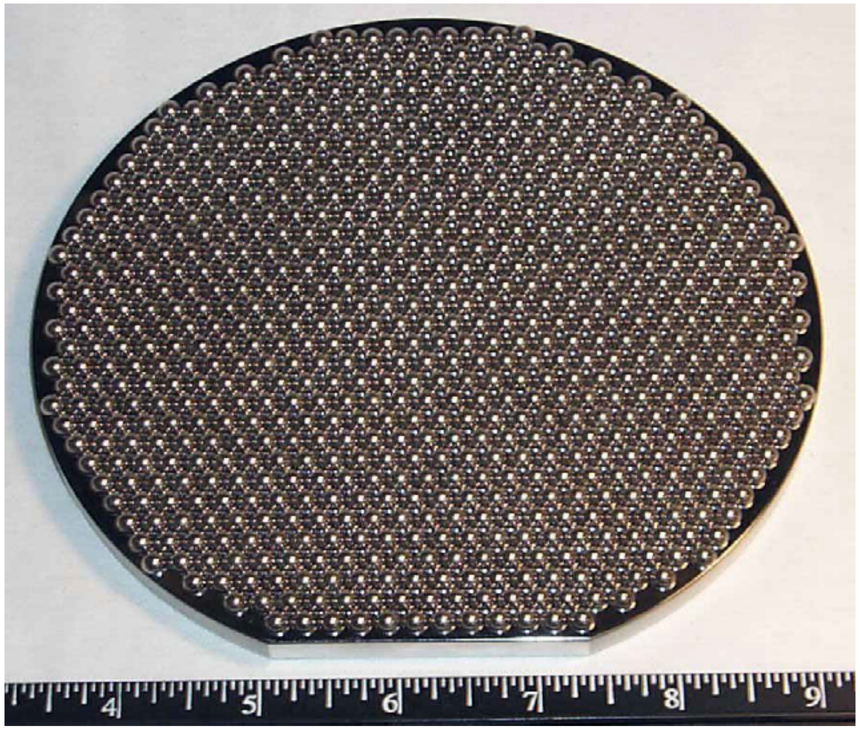

Test Apparatus (M. Myers)

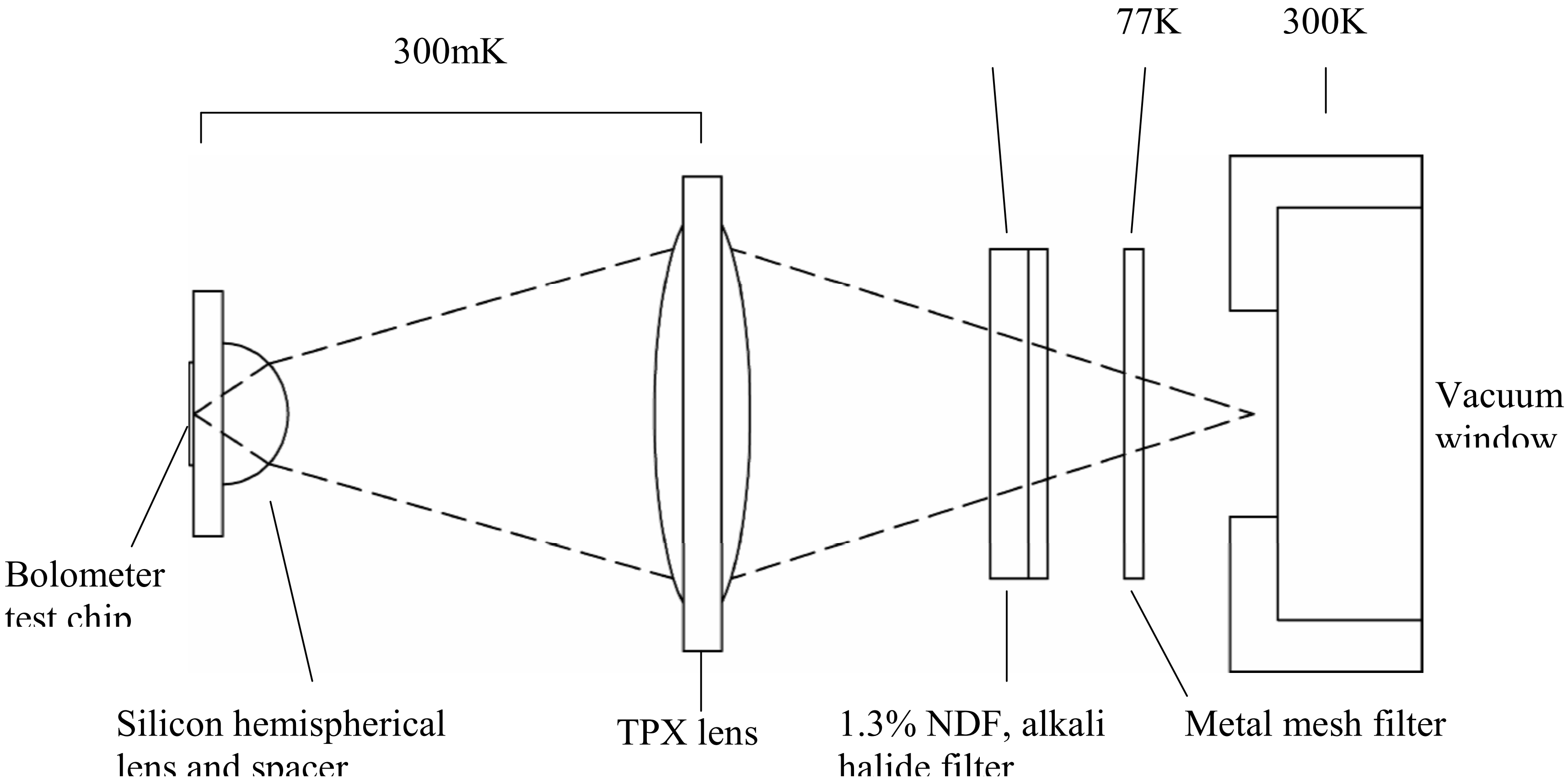

Test Apparatus (Mike Myers, Dan Schwan)

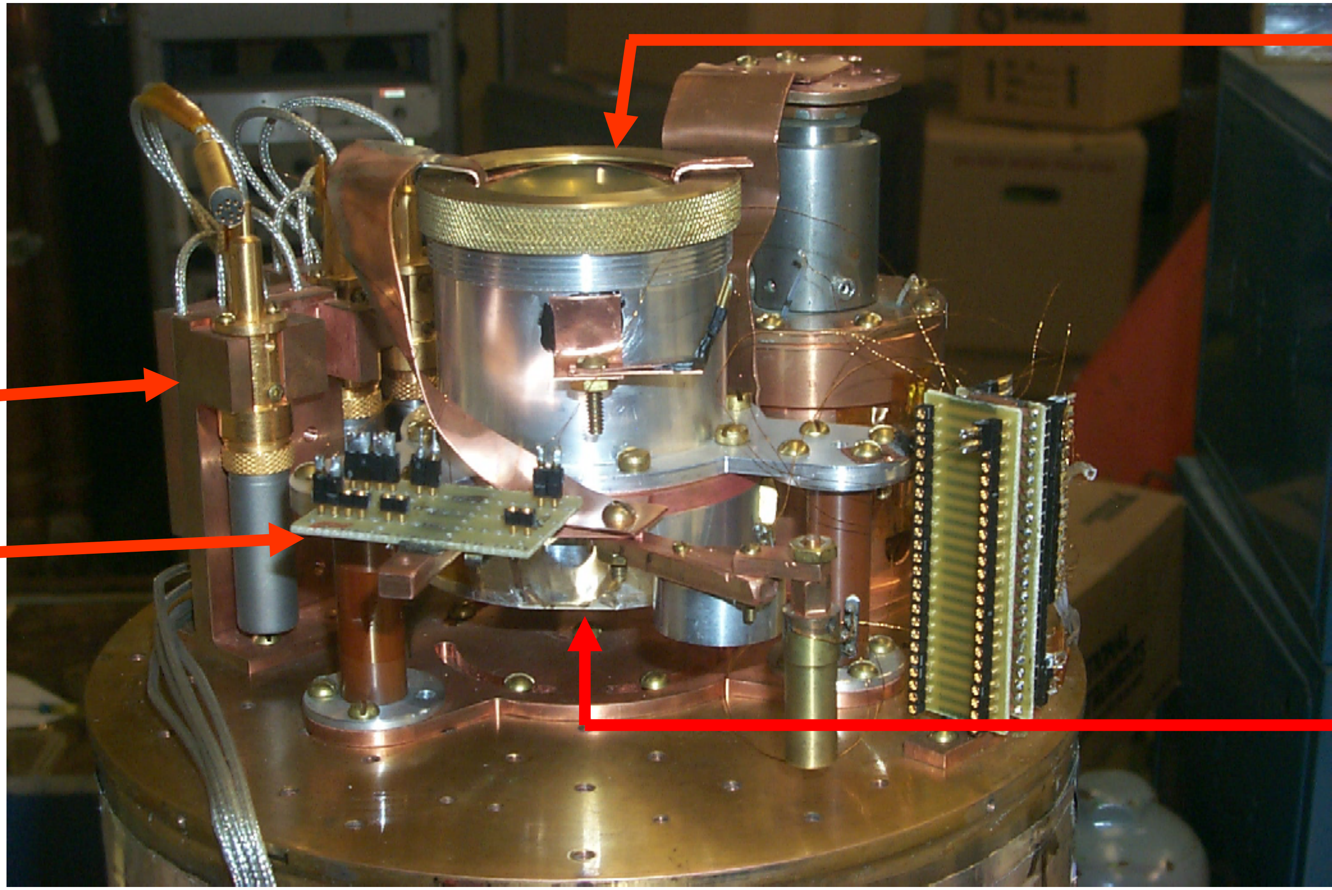

Typical parameters:

- $G \sim 9 \times 10^{-10}$ W/K
- Expected white noise from < 1 Hz to 100 Hz (thermal fluctuation limit)
- $T_C \sim 450$mK
- $\tau \sim 0.2 - 0.3$ ms
- $R_{load} \sim 25\ \Omega$ ($10\ \Omega$ design value)

Preliminary results

- Polarization sensitivity

  Chopped LN load and wire grid polarizer
  Cross polarization 3% upper limit

- Rough beam map
  ~ 4° symmetric beam, matches expectation

Frequency Response (optical transmission)

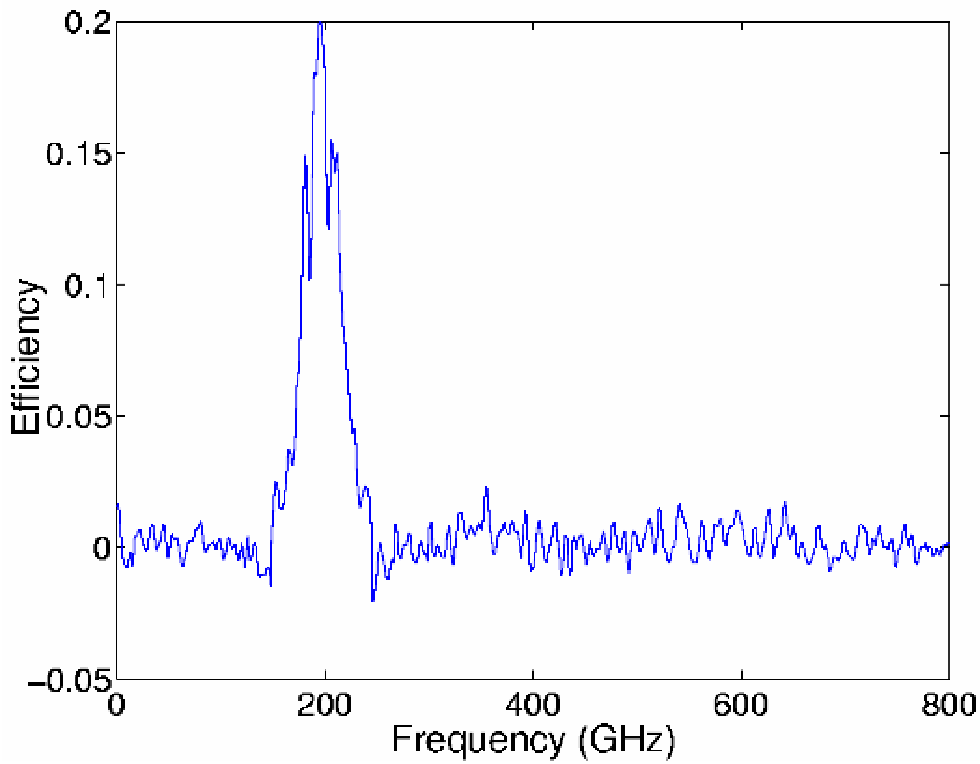

Performance adequate, but not optimized

x2 improvement expected (no anti-reflective coating yet)
(for comparison: Planck spec is 30% efficiency)

Readout

Heat leaks through connecting wires from 0.25K bolometer stage to 4K SQUID stage are prohibitive for large arrays

Solution: Multiplexing

Constraints: Low impedance required to maintain constant voltage bias

Power budget at 0.25K stage <1 μW

Two options:

Time domain multiplexing (NIST, K. Irwin et al.)

1 SQUID per bolometer

Frequency domain multiplexing

LBNL design: 1 SQUID reads out ~30 bolometers

More bolometers possible: discussion later

Principle of Frequency-Domain Multiplexing

1. AC bias bolometers (~100 kHz – 1 MHz)

   each bolometer biased at different frequency

2. Signals change sensor resistance

   ⇒ modulate current

   ⇒ transfer signal spectrum to sidebands adjacent to bias frequency

   ⇒ each sensor signal translated to unique frequency band

3. Combine all signals in common readout line

4. Retrieve individual signals in bank of frequency-selective demodulators

Modulation Basics

If a sinusoidal current $I_0 \sin \omega t$ is amplitude modulated by a second sine wave $I_m \sin \omega_m t$

$$I(t) = (I_0 + I_m \sin \omega_m t) \sin \omega t$$
$$I(t) = I_0 \sin \omega t + I_m \sin \omega_m t \sin \omega t$$

Using the trigonometric identity $2 \sin \alpha \sin \beta = \cos(\alpha - \beta) - \cos(\alpha + \beta)$ this can be rewritten

$$I(t) = I_0 \sin \omega t + \frac{I_m}{2} \cos(\omega t - \omega_m t) - \frac{I_m}{2} \cos(\omega t + \omega_m t)$$

The modulation frequency is translated into two sideband frequencies $(\omega t + \omega_m t)$ and $(\omega t - \omega_m t)$ symmetrically positioned above and below the carrier frequency ω.

All of the information contained in the modulation signal appears in the sidebands; the carrier does not carry any information whatsoever.

The power contained in the sidebands is equal to the modulation power, distributed equally between both sidebands.

MUX circuit on cold stage

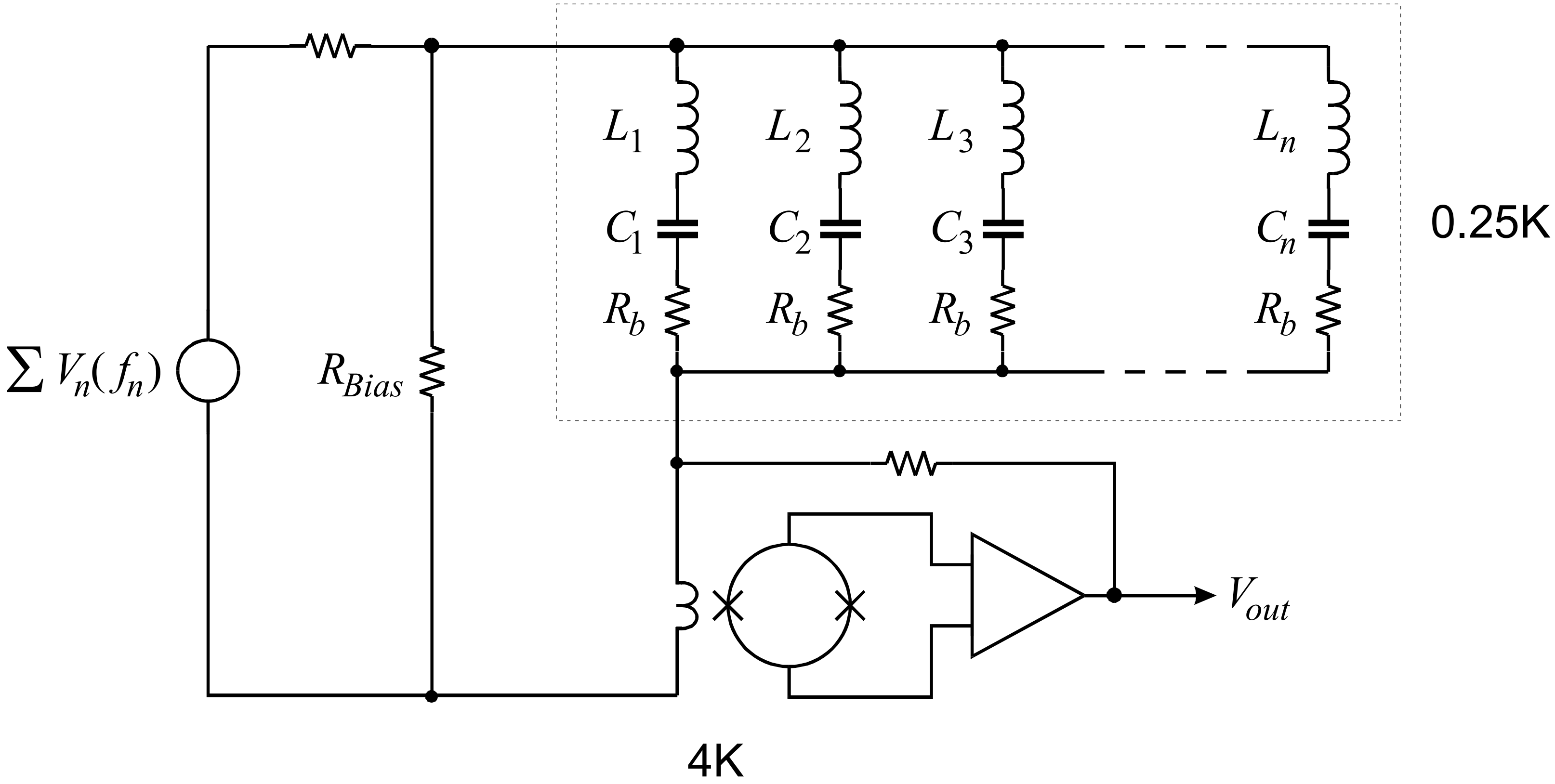

"Comb" of all bias frequencies fed through single wire
Tuned circuits "steer" appropriate frequencies to bolometers
Current return through shunt-fedback SQUID amplifier (low input impedance)
No additional power dissipation on cold stage (only bolometer bias power)

Demodulation

The same carrier signal that biases the sensor is used to translate the sideband information to baseband.

The mixer acts analogously to a modulator, where the input signal modulates the carrier, forming both sum and difference frequencies.

In the difference spectrum the sidebands at $f_n \pm \Delta f_S$ are translated to a frequency band

$$f_n - (f_n \pm \Delta f_S) = 0 \pm \Delta f_S .$$

A post-detection low-pass filter attenuates all higher frequencies and determines the ultimate signal and noise bandwidth.

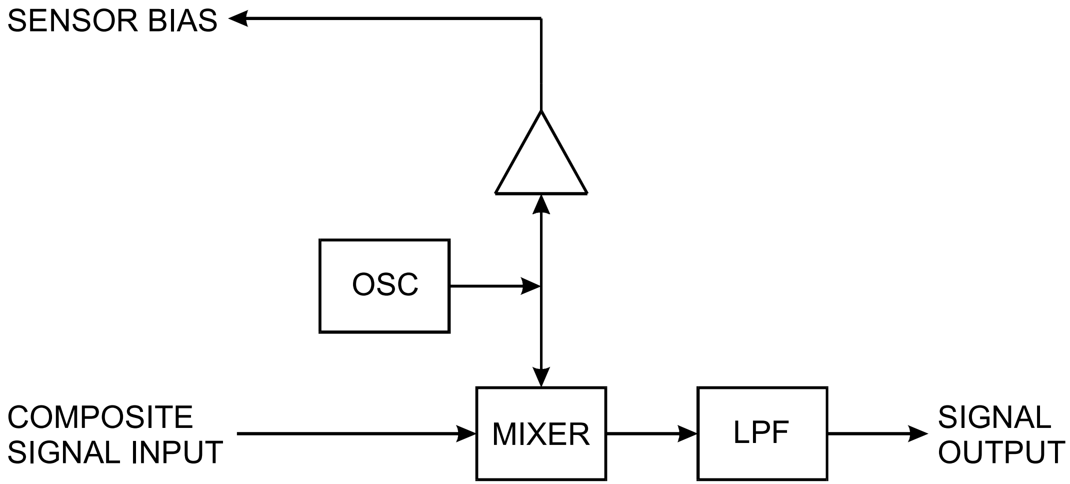

System Block Diagram

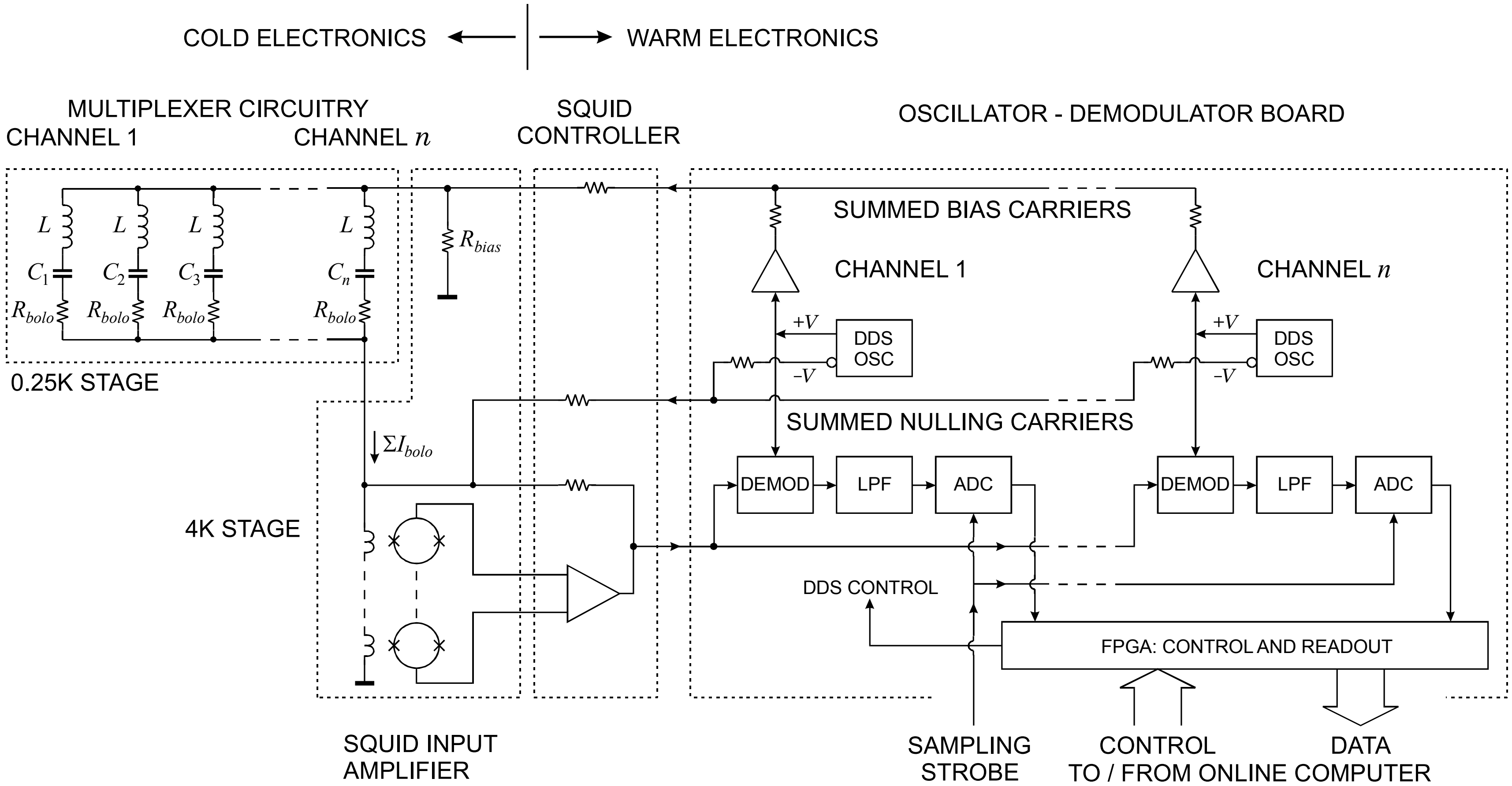

Intermodulation

SQUID output voltage approx. sinusoidal function of flux $\Rightarrow$ non-linear: $\sin x \approx x - \frac{x^3}{3!} + \frac{x^5}{5!}$ ...

Non-linear terms lead to mixing products.

For two input frequencies f_1 and f_2: 3rd order distortion $\Rightarrow$ $3 f_1$

$3 f_2$

$2 f_1 \pm f_2$

$2 f_2 \pm f_1$

What levels are of concern?

Bolometer noise current: 10 pA/Hz$^{1/2}$
Bandwidth: 1 kHz
Total noise current: 320 pA

Bolometer bias current: 10 μA

i_{noise} / i_{bias} = $3.2 \cdot 10^{-5}$ (-90 dBC)

Depends on ratio of signal to max optical loading

System must be designed for very low distortion – choose appropriate technology

Similar constraint applies to all frequency multiplexing schemes

Carrier Nulling

All of the information is in the sidebands, so the carrier can be suppressed to reduce dynamic range requirements.

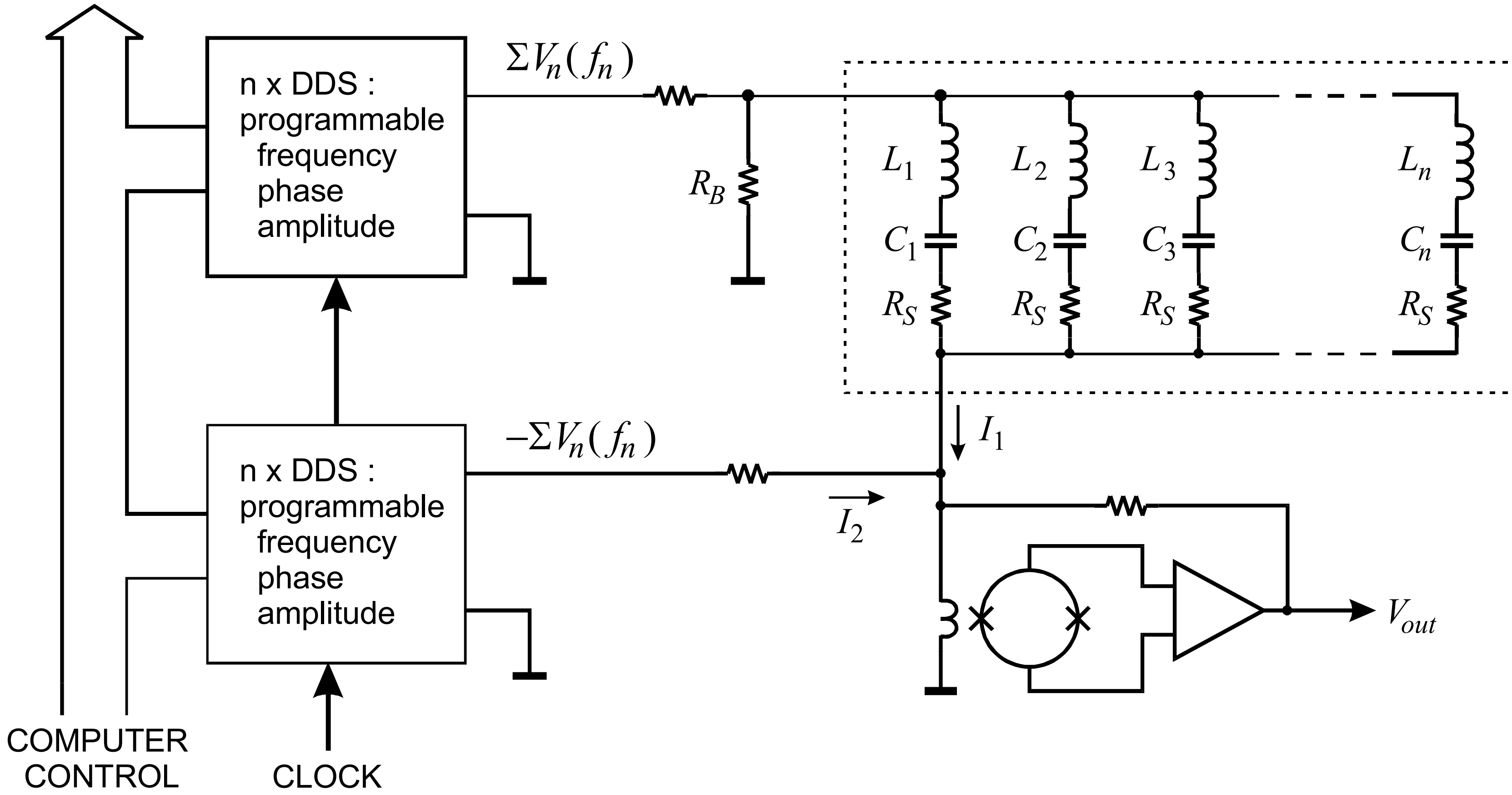

How many bolometers can be MUXed?

1. Frequency spacing of bias carriers depends on selectivity of tuned circuits.

2. Minimum LC bandwidth (Q) set by bolometer time constant.

3. Channel spacing set by allowable cross-talk and noise leakage from other channels.

4. Minimum frequency set by bolometer thermal time constant
   (typ. min. 100 kHz)

5. Maximum frequency set by large-signal bandwidth of SQUID feedback loop.

   Loop gain-bandwidth product: set by a) required dynamic range
   (no. and magnitude of carriers)
   b) distortion in SQUID

   Limited by total wiring length of feedback loop

   Example: round trip wiring length of 20 cm limits loop gain-bandwidth product
   to ~100 MHz (at 1 MHz extend dynamic range x100)

H. Spieler, Frequency Domain Multiplexing for Large-Scale Bolometer Arrays, in Proceedings Far-IR, Sub-mm & mm Detector Technology Workshop, Wolf J., Farhoomand J. and McCreight C.R. (eds.), NASA/CP-211408, 2002 and LBNL-49993, www-physics.LBL.gov/~spieler.

Solutions

1. Maximize dynamic range of SQUID

   SQUID is limited by flux, so reducing the mutual input inductance allows larger input current.

   Smaller input mutual inductance
   increases input noise current
   reduces SQUID transresistance (gain)

   Limited by bolometer noise and noise of warm amplifier

   $\Rightarrow$ SQUID arrays (many SQUIDs connected in series)

   We use 100-SQUID arrays from NIST

2. Cold feedback loop

   Use cryogenic Si MOSFET or GaAs MESFET amplifier at 4K
   Reduced wire length increases maximum frequency.

With SQUID array and cold/warm feedback loop ~30 channels per readout line practical.

Hardware

1st generation prototypes tested end-to-end with bolometers

Now fabricating production prototypes
(APEX-SZ, SPT, PolarBear use similar designs)

Focal Plane Assembly

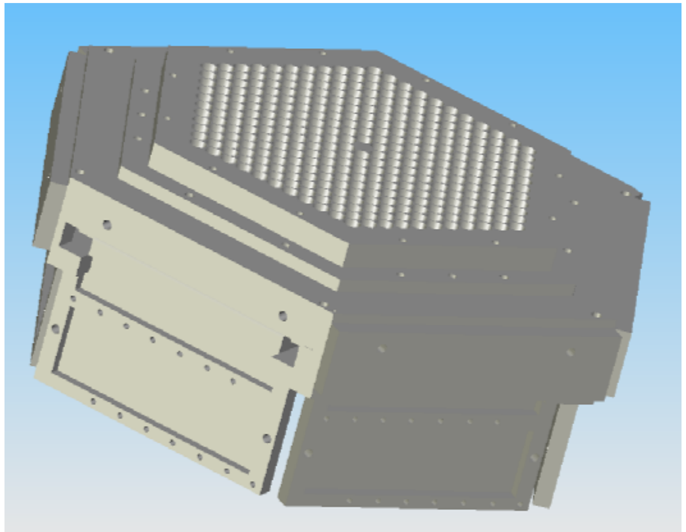

Layout of flex interconnect from bolometer array to wiring harness to SQUIDs

G10

Kapton flex

G10

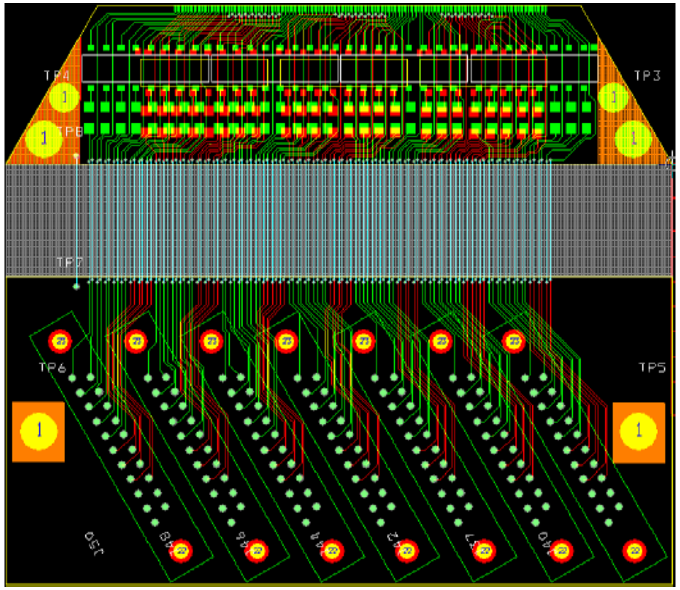

(Z. Kermish)

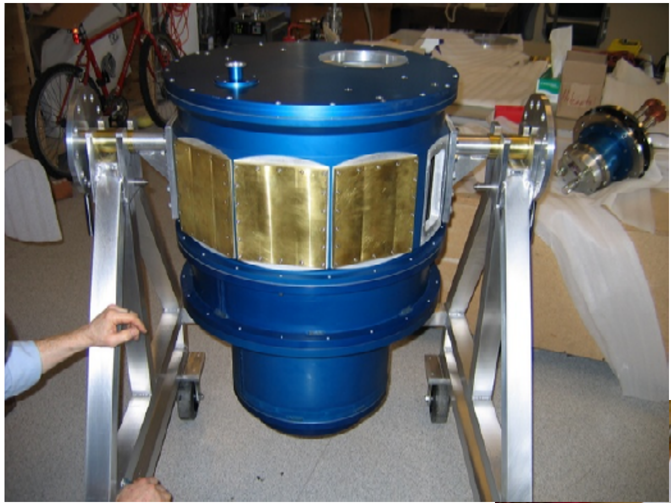

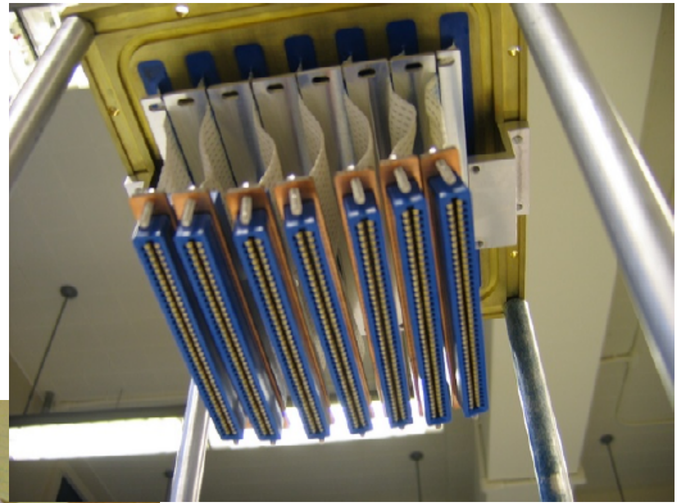

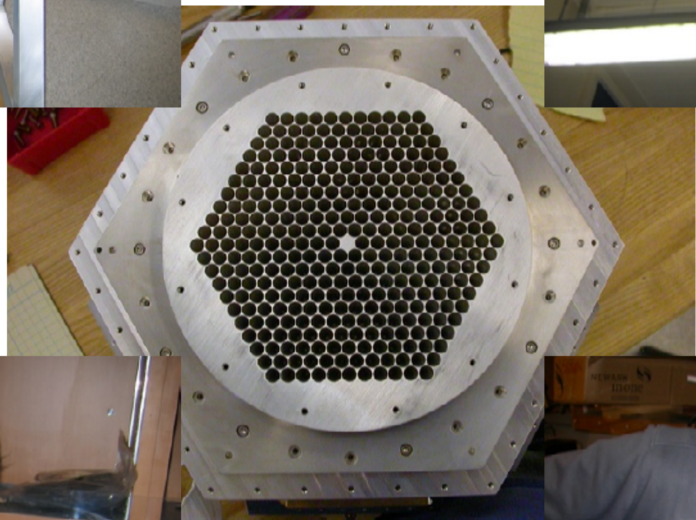

MUX chip (0.25K stage)

Superconducting spiral inductors

integrated on a chip

5 mm

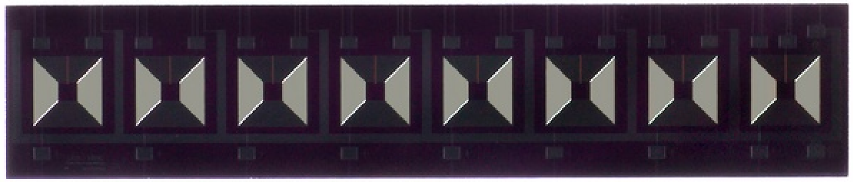

(fabbed by Northrup-Grumman)

Capacitors can be integrated with inductors, but external chip capacitors require less space.

NP0 capacitors perform well at 4K

SQUIDs mounted as arrays of eight in magnetic shield (4K stage)

SQUID mounting board

SQUIDs mounted on Nb pads
to pin magnetic flux

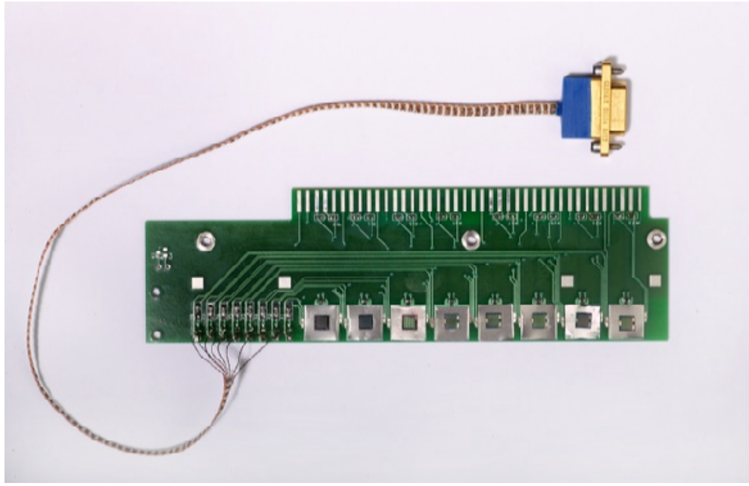

Magnetic Shield
(M. Lueker)

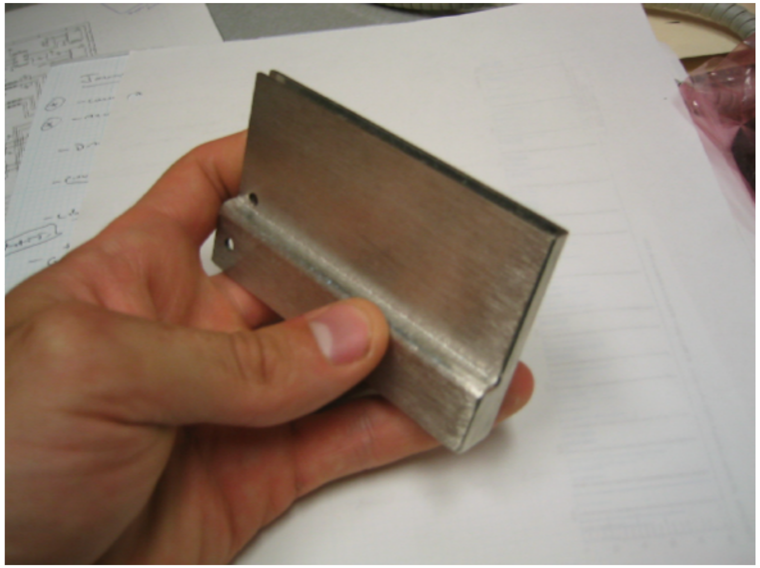

8-channel SQUID Controller

Computer-controlled
SQUID diagnostics
Open/closed loop
Switchable gain

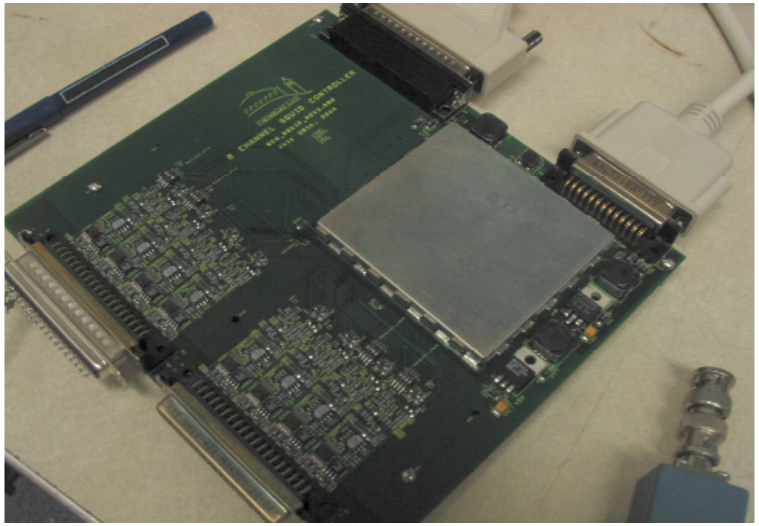

16-channel Demodulator Board

16 individual demodulator channels
2 DDS freq. generators per channel
(bolometer bias + carrier nulling)
on-board A/D
opto-isolated computer interface

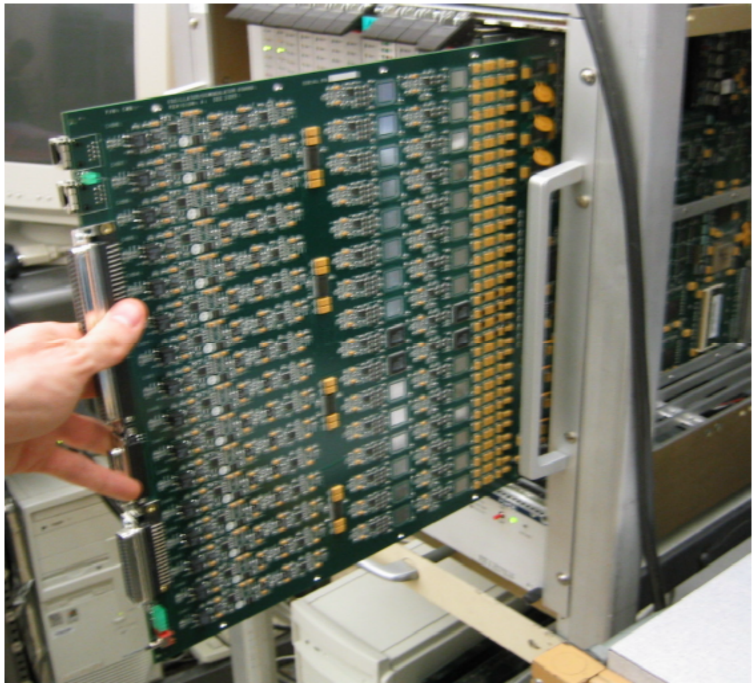

Design and prototyping at LBNL
(M. Dobbs, J. Joseph, M. Lueker, C. Vu)

MUX measurements using 1st generation boards (T. Lanting)

Bias comb sent to SQUID (top) and measured at SQUID output (bottom)

8-channel MUX

- 7 bolometers
- + one dummy resistor

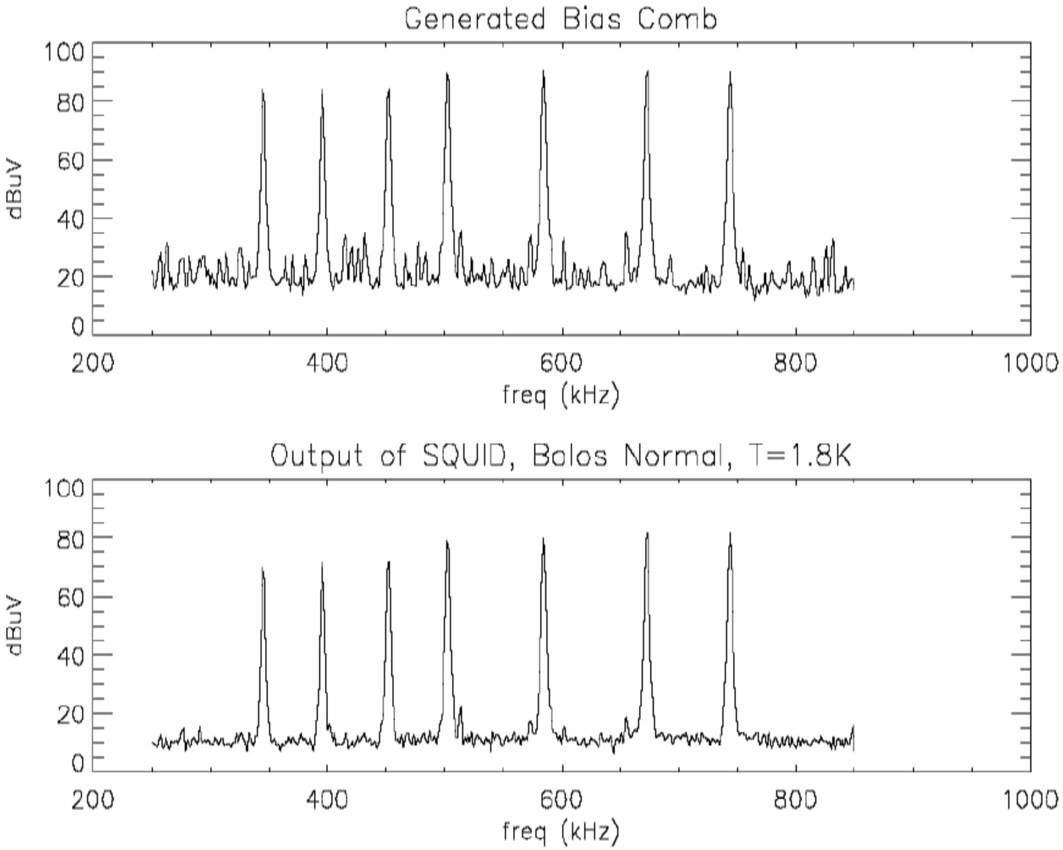

Measured noise agrees with theory

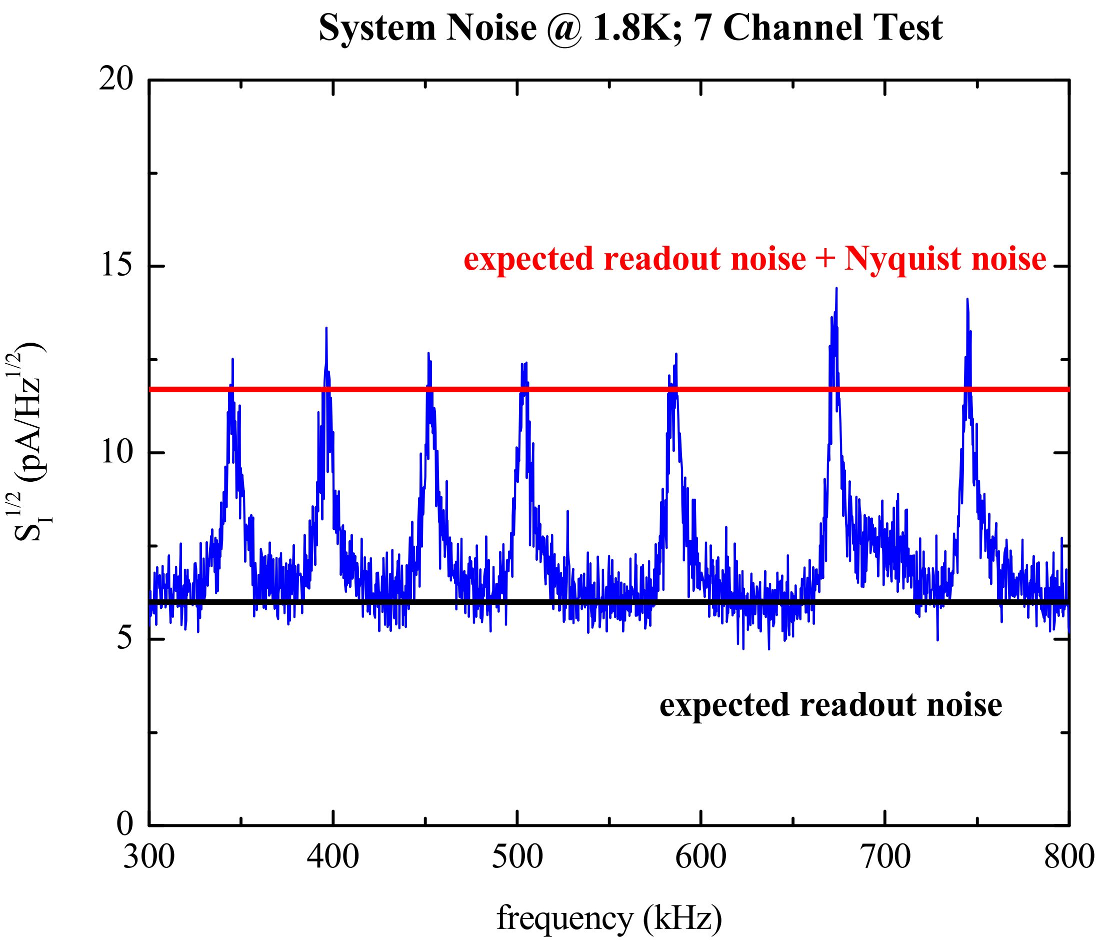

Cross-Talk <0.8% (in agreement with design simulation)

One bolometer illuminated by modulated LED

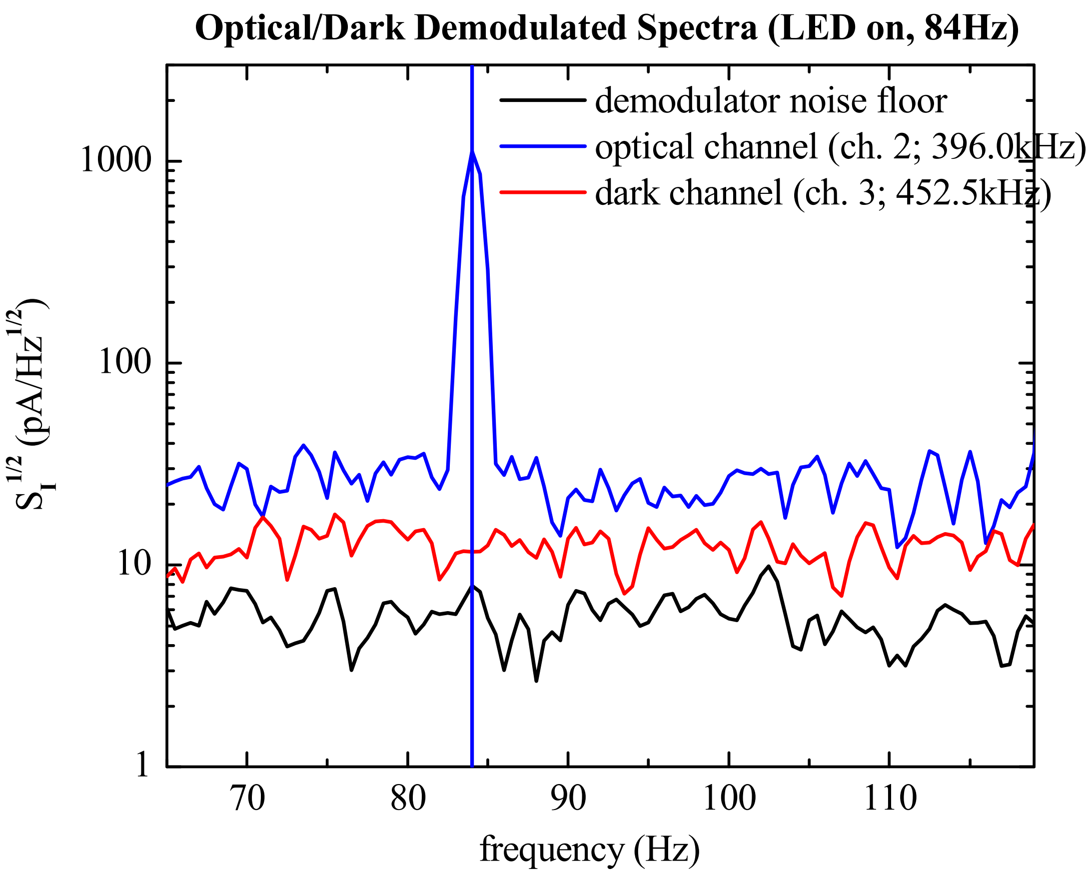

Measured Noise Spectrum (preliminary measurement valid >0.1Hz)

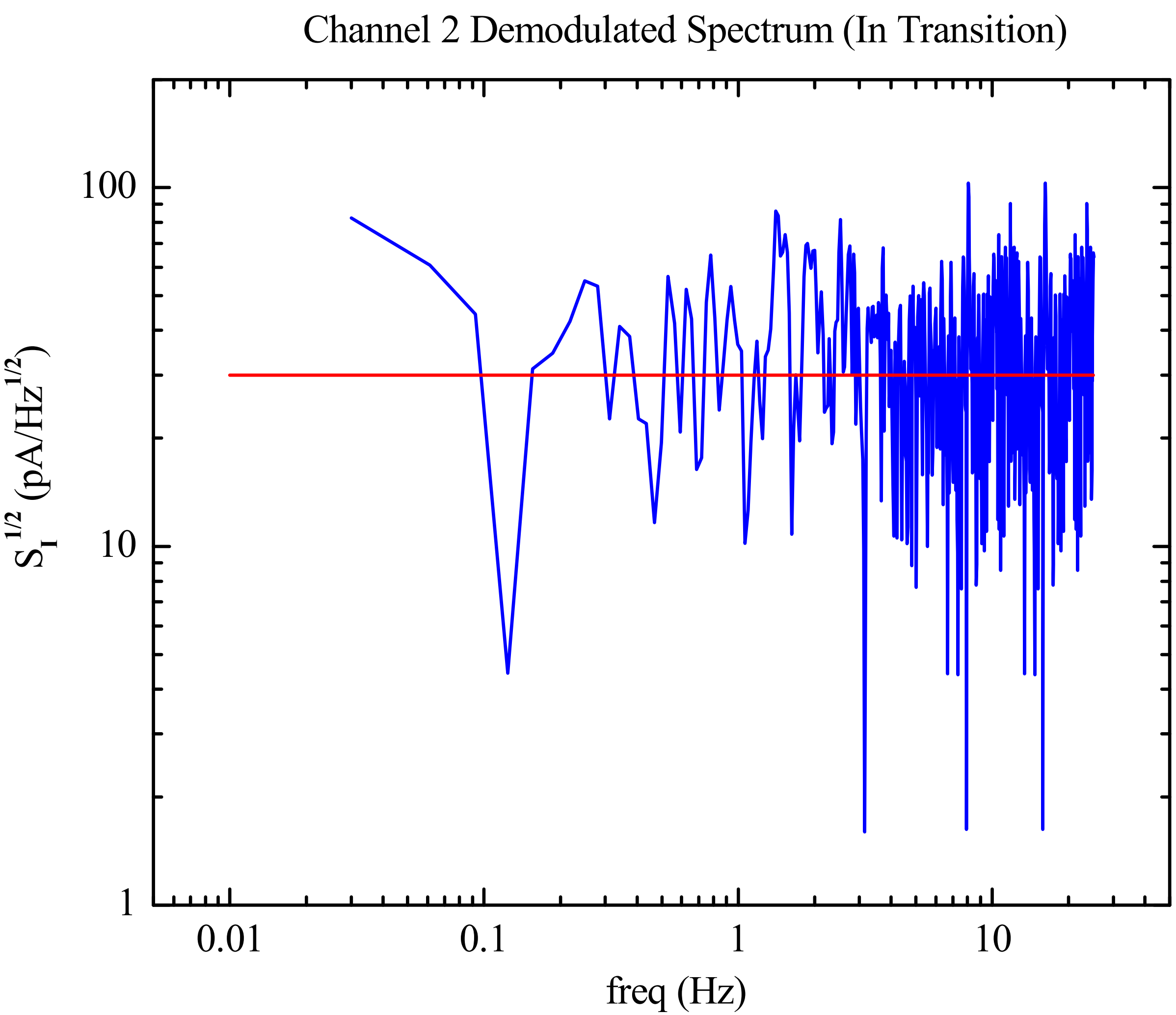

Frequency-Domain MUX Demonstrated with X-Ray Micro-Calorimeters

LLNL/UCB/LBNL collaboration

Time domain

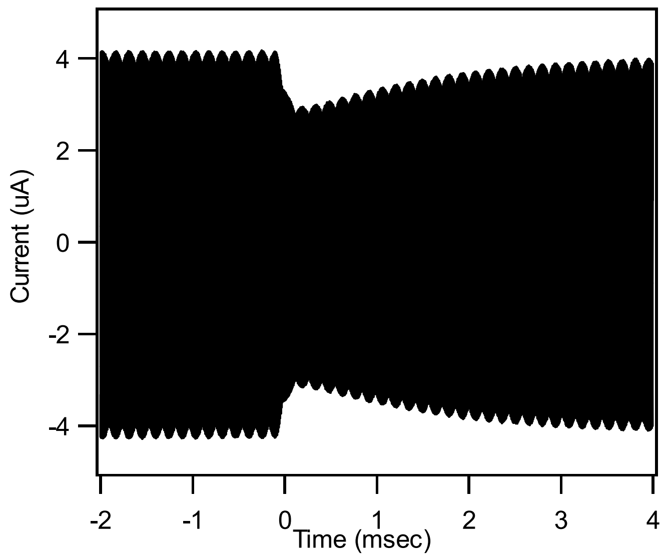

Frequency Domain

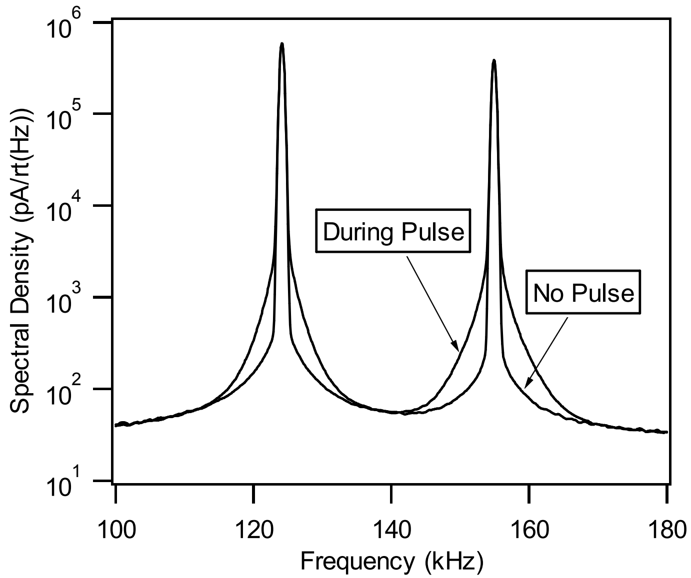

Energy resolution of 60 eV FWHM unaffected by multiplexer.

MUXing $\Rightarrow$ increase active area, overall rate capability

Summary: Breakthrough in Cryogenic Detectors

- Sensitivity approaching quantum level at mm wavelengths
- Voltage-biased superconducting transition edge sensors

  ⇒ stable operation
  predictable response

- Sensors can be fabricated using monolithic technology developed for Si integrated circuits, micro-mechanics

  ⇒ economical fabrication of large sensor arrays

- Challenge: Readout
  (multiplexing of many channels)

  production prototypes tested successfully, but still much work to do

- great opportunities for students + post-docs!

Exciting Times in Physics!

- Dark Matter and Dark Energy comprise 95% of the universe.
- We don't know what the dark matter is, nor do we have any credible explanation of dark energy.
- All of the physics and chemistry of the past ~400 years has been directed at understanding only 5% of the universe!
- We may find the "new physics" by looking 13 billion years into the past.

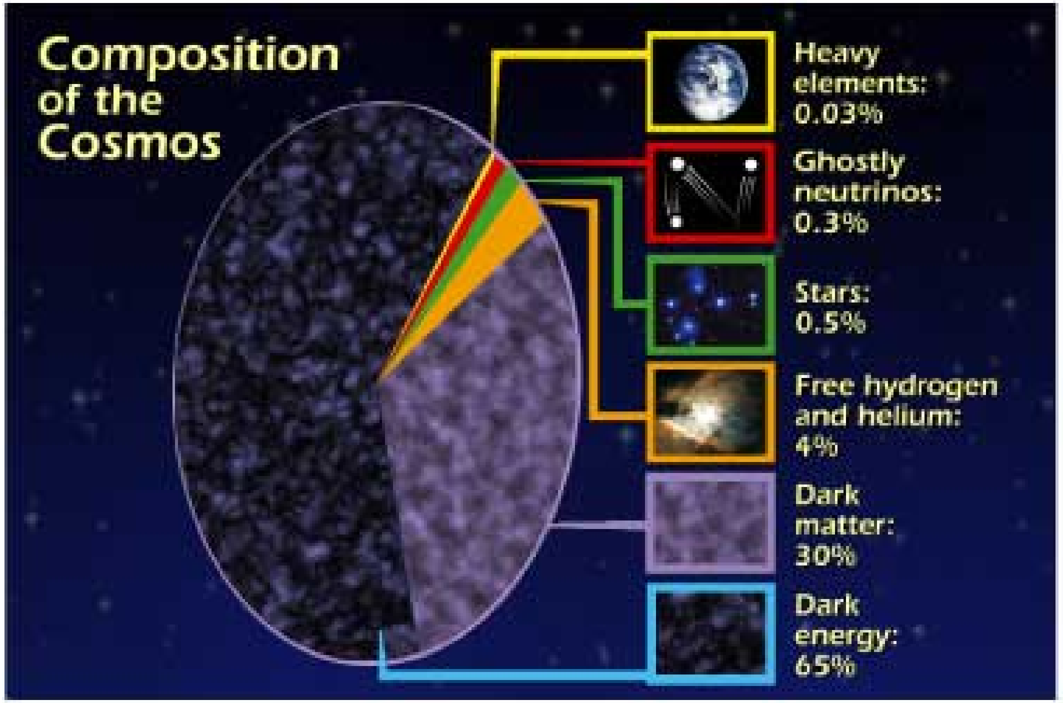

- One thing is clear - new detectors will play a key role in solving these mysteries.